Inorganic Chemistry

ARTICLE

pubs.acs.org/IC

Synthesis and Characterization of Neutral Luminescent Diphosphine Pyrrole- and Indole-Aldimine Copper(I) Complexes

Marco G. Crestani, Gerald F. Manbeck, William W. Brennessel, Theresa M. McCormick, and Richard Eisenberg*

Department of Chemistry, University of Rochester, Rochester, New York 14627, United States

Supporting Information

ABSTRACT: Heteroleptic copper(I) complexes of the types [Cu(N,N)(P,P)] and [Cu(N,O)(P,P)], where (P,P) = phosphine (PPh_3) or diphosphine (dppb, DPEPHOS, XANTPHOS), (N,N) = pyrrole-2-phenylcarbaldimine, **2PyN**: [Cu(2PyN)(PPh_3)$_2$] (**1**), [Cu(2PyN) (dppb)] (**2**), [Cu(2PyN)(DPEPHOS)] (**3**), and [Cu(2PyN)(XANTPHOS)] (**4**), (N,N) = indole-2-phenylcarbaldimine, **2IndN**: [Cu(2IndN)(DPEPHOS)] (**8**), and (N,O) = pyrrole-2-carboxaldehyde, **2PyO**: [Cu(2PyO)(DPEPHOS)] (**5**), [Cu(2PyO)(XANTPHOS)] (**6**), or (N,O) = indole-2-carboxaldehyde, **2IndO:** [Cu(2IndO)(DPEPHOS)] (**7**), were synthesized and characterized by multinuclear NMR spectroscopy, electronic absorption spectroscopy, fluorescence spectroscopy, and X-ray crystallography (**1**−**3**, **5**−**8**). The complexes with aldimine ligands are thermally stable, and sublimation of **2**−**4** was possible at T = 230−250 °C under vacuum. All complexes exhibit long-lived emission in solution, in the solid state, and in frozen glasses. The excited states have been assigned as mixed intraligand and metal-to-ligand charge transfer ^{3}(MLCT + π−π^*) transitions through analysis of the photophysical properties and DFT calculations on representative examples.

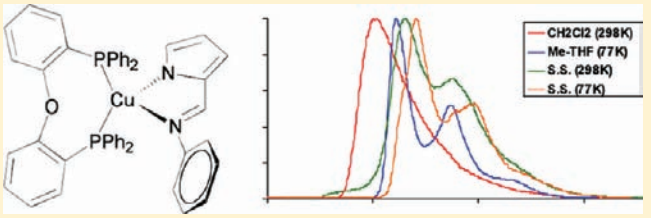

INTRODUCTION

The search for low-cost, highly efficient emitters for the manufacture of organic light-emitting diodes (OLEDs) is considered of great importance given the potential that OLEDs have for flat panel displays and solid-state lighting.[1] OLEDs are current-driven devices and in their simplest form are comprised of an anode (hole injection), a cathode (electron injection), and an organic medium that is sandwiched between the two electrodes to support charge recombination that yields emission of light.[2] To improve the power efficiency of the device, phosphorescent emitters are doped into a polymer matrix of the OLED, thereby allowing access to emissive triplet excitons which would otherwise be lost as heat in organic emitters.[3] OLED fabrication may be done by solution processing or vapor deposition. Solution processing is attractive for its low cost, whereas vapor deposition generally offers more options in multilayer device fabrication by eliminating problems, such as dissolution of underlying layers during solution processing of succeeding layers. Thus, in addition to high luminescence quantum efficiency, thermal stability and sublimability are required properties of emitters for vapor-deposited OLEDs.

Cyclometalated d^6 and d^8 complexes of the third row transition series, especially iridium(III), have been employed with the most success in OLEDs because of their high phosphorescence quantum yield, wavelength tunability, and thermal stability.[4] However, because of the high cost and limited availability of these precious metals, extensive efforts have been directed toward the discovery of less expensive alternatives,[5] especially copper(I) complexes.[6] Many of the complexes employed have been of the type [Cu(NN)(PP)]$^+$ (NN = diimine and PP = diphosphine),[6c−f,i−l] following the seminal advances made by McMillin and co-workers in the design of such complexes for higher photoluminescence quantum yields.[7] The cationic nature of these complexes usually would preclude device fabrication by vapor deposition, but nonetheless several cases of vapor-deposited OLEDs have been reported.[6c,d,i] A few studies of vapor-deposited OLEDs have appeared using neutral, sublimable Cu(I) complexes,[6a,b,h] including the highly emissive dinuclear Cu(I) complex, [Cu(PNP)]$_2$ (PNP = bis(2-diisobutylphosphinophenyl)amide).[6b] A novel device fabrication method involving codeposition of Cu(I) with coordinating ligands to form emissive complexes in situ has also been reported.[6a] Previous work in our laboratory has focused on neutral Cu(I) complexes supported by diphosphine and amidotriazole ligands, but their thermal instability prevented practical device application.[8]

In the current work, we have prepared heteroleptic neutral copper(I) compounds of the types [Cu(N,N)(P,P)] and [Cu(N,O)(P,P)] ((P,P) = 2 PPh_3 or a diphosphine (see Scheme 1), (N,N) = pyrrole-2-phenylcarbaldimine, **2PyN**, or indole-2-phenylcarbaldimine, **2IndN**, and (N,O) = pyrrole-2-carboxaldehyde, **2PyO**, or indole-2-carboxaldehyde, **2IndO**) that could be employed for the construction of OLED devices by vacuum deposition. Our choice of using pyrrole-aldimine derivatives as ligands was motivated by the use of thermally stable homoleptic

Received: April 12, 2011
Published: June 29, 2011

Scheme 1. Phosphine (PPh_3) and Diphosphines (P,P) Used in This Work: PPh_3 = Triphenylphosphine, dppb = 1,2-Bis(diphenylphosphino)benzene, DPEPHOS = (Oxydi-2,1-phenylene)bis-diphenylphosphine, XANTPHOS = 9,9-Dimethyl-4,5-bis(diphenylphosphino)xanthene

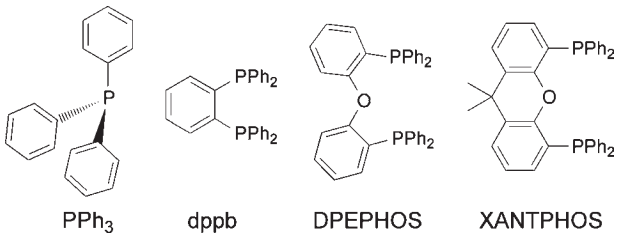

copper(II) bis-pyrrole-2-phenylcarbaldimine compounds for Cu metal deposition via a CVD/ALD (CVD = chemical vapor deposition; ALD = atomic layer deposition) process.[9] The pyrrole-aldehyde congeners were prepared for comparison of their photophysical properties to those of pyrrole-aldimine complexes. The indole derivatives (both with aldimine and aldehyde functions) were studied to determine the effect of extended conjugation on photoluminescence. In addition, the use of pyrrole-aldimine ligands for the synthesis of the copper(I) compounds was encouraged by literature precedents that showed that this type of ligand is a useful scaffold for the preparation of luminescent Zn(II) compounds and other coordination complexes,[10,11] although the short-lived singlet emission in these complexes makes them unsuited for triplet harvesting in OLED devices.[10b] To our knowledge, emissive indole-based copper(I) complexes have not been described in the literature.

EXPERIMENTAL SECTION

General Considerations. Unless otherwise noted, all manipulations in this work were performed using standard Schlenk and glovebox techniques under a nitrogen atmosphere. A double VAC inert-atmosphere glovebox was used. Glassware was oven- or flame-dried and cooled to room temperature under dynamic vacuum.

Materials and Methods. All of the solvents used were reagent grade. Dichloromethane (CH_2Cl_2), tetrahydrofuran (THF), hexanes, and diethyl ether were dried and purified by filtration through activated-alumina columns using a solvent purifier.[12] Acetonitrile (MeCN) was dried over calcium hydride (CaH_2). Ethanol and methanol were dried over calcium sulfate ($CaSO_4$). Toluene was distilled over sodium. 2-Methylfuran (2-Me-THF, 99% stabilized with ca. 150−400 ppm of BHT) was distilled from sodium/benzophenone ketyl.[13] All of the water used was deionized. Isopropyl alcohol was used as received. d_2-Dichloromethane (CD_2Cl_2) and d_1-chloroform ($CDCl_3$) were purchased from Cambridge Isotope Laboratories (CIL, Andover, MA), degassed by freeze−pump−thaw (FPT), and stored over activated 3 Å molecular sieves. CuCl (Aldrich, 98%), pyrrole-2-carboxaldehyde (**2PyO-H**; Aldrich, 98%), indole-2-carboxaldehyde (**2IndO-H**; TCI America, 97%), aniline ($PhNH_2$; Aldrich, 97%), triphenylphosphine (PPh_3; Aldrich, 99%), 1,2-bis(diphenylphosphino)benzene (dppb; Aldrich, 97%), (oxidi-2,1-phenylene)bis-diphenylphosphine (DPEPHOS; 98%, Aldrich), 9,9-dimethyl-4,5-bis(diphenylphosphino)xanthene (XANTPHOS; ACROS organics, 98%), and potassium *tert*-butoxide (KO^tBu; Aldrich, 95%) were purchased in high purity grade and used as received. $[Cu(NO_3)(PPh_3)_2]$ was prepared following the literature procedure.[14] Purities of all products were confirmed by microanalyses carried out by Quantitative Technologies, Inc. (QTI, Whitehouse, NJ). Thin-wall (0.38 mm) WILMAD screw-capped NMR tubes were used for both NMR spectroscopy and low-temperature fluorimetry. Quartz cells (Starna Cells, Inc., Atascadero, CA) were used for recording room temperature absorption and emission spectra of fluid solutions.

^1H (400, 500 MHz), $^{13}C\{^1H\}$ (100, 125 MHz), and $^{31}P\{^1H\}$ (162, 202 MHz) NMR spectra were recorded on Bruker Avance 400 and Avance 500 spectrometers. ^1H and $^{13}C\{^1H\}$ chemical shifts (δ, ppm) are reported relative to the residual proton or carbon resonances of the deuterated solvent. $^{31}P\{^1H\}$ NMR spectra are reported in ppm relative to external 85% H_3PO_4. UV/visible absorption spectra were recorded using quartz cuvettes in a Hitachi U2000 scanning spectrophotometer (200−1100 nm), at 298 K. Excitation and emission spectra of fluid solutions (298 K), solid-state samples, and frozen glasses (77 K) were recorded using a Spex Fluoromax-P fluorimeter. All fluid-solution spectra were measured using freshly prepared samples, deoxygenated by FPT. Emission spectra were corrected for the spectral sensitivity of the photomultiplier tube and the spectral output of the lamp. Extinction coefficients (ε, M^{-1} cm^{-1}) of all the copper compounds and their deprotonated ligands were determined from their corresponding Beer's plots at three different concentrations (5, 3, and 1 × 10^{-5} M; see Supporting Information). The relative emission quantum yields (Φ_{em}) were determined in fluid dichloromethane solution (refractive index, η = 1.4242), following the method of Demas and Crosby for optically dilute solutions,[15] according to the formula $\Phi_{em} = \Phi_f = \Phi_R(I_R/I_f)(\eta_f^2/\eta_R^2)(D_f/D_R)(A_R/A_f)$, where I is the excitation intensity ($(I_R/I_f) \sim 1$), η is the refractive index of the solution, D = integrated emission intensity, and A is the absorption at the excitation wavelength for the standard reference (R) and the sample (f), respectively.[16] An aerated aqueous solution of tris(2,2′-bipyridyl)ruthenium(II) ion, $[Ru(bipy)_3]^+$, (η = 1.333, Φ = 0.028) was used as the standard.[17] The emission spectra of each sample and of the reference were recorded at the same excitation wavelength (λ_{ex} nm) under identical instrument configurations for all Φ_{em} determinations. Concentrations of both the sample and the reference were then adjusted to match an absorbance of 0.1 at the excitation wavelength, and the resulting emission spectra were integrated. At least three independent measurements were performed for each determination. Closed-cap NMR tubes charged with Me-THF solutions of the copper(I) compounds under nitrogen were used to record low-temperature emission and excitation spectra. Flame-sealed capillaries were used for solid state samples. Lifetime data were collected using the Spex Fluoromax-P fluorimeter in phosphorimeter mode. Spectra were obtained after a 10 ms flashlamp delay, and decay curves were collected as the average of 5 runs. Data were fit to appropriate exponential or biexponential decay equations.

Sublimation Experiments. Laboratory-scale sublimations were performed using a cylindrical glass microsublimator. Samples (0.050 g) of three copper(I) compounds (**2**, **3**, **4**) were tested in separate runs. The sublimator was charged in a glovebox and further heated under vacuum on a Schlenk line. Heating was maintained using a mantle until sublimation of the material was observed. For compounds **2** and **3**, sublimation occurred at 230 °C. In the case of **4**, sublimation took place at 250 °C. The typical yield of sublimation was 40% (0.020 g).

Preparation of [N,N] Ligand Precursors. *Pyrrole-2-phenylcarbaldimine (**2PyN-H**).* This compound was prepared according to the literature[18] in 98% yield and recrystallized from ethanol/hexanes (1:5 v/v).

*Indole-2-phenylcarbaldimine (**2IndN-H**).* A mixture of 2-indolealdehyde (0.2496 g, 1.7 mmol) and aniline (0.16 mL, 1.7 mmol) in water (15 mL) was refluxed for 12 h. The mixture was cooled and partitioned between CH_2Cl_2 and water. The aqueous layer was washed 3 times with CH_2Cl_2. The organic portions were combined and dried over $MgSO_4$, filtered, and concentrated. The resulting dark red solid was recrystallized from ethanol/hexanes (1:5% v/v). The yield of **2IndN-H** was 0.3517 g (1.6 mmol, 94.1%) of dark red-brown microcrystals. ^1H NMR (500 MHz, CD_2Cl_2): δ/ppm 9.63 (*br s*, 1H, N−*H*), 8.59 (*s*, 1H, C*H*=N), 7.75 (*dd*, J_1 = 8 Hz, J_2 = 1 Hz, 1H, indole C−*H*), 7.52−7.45 (*m*, 3H, *m*-aryl, and indole C−*H*), 7.38−7.32 (*m*, 4H, *o*-, *p*-aryl, and indole C−*H*),

dx.doi.org/10.1021/ic2007588 |*Inorg. Chem.* 2011, 50, 7172–7188

7.198 (*m*, 1H, indole C−*H*), 7.08 (*dd*, J_1 = 2 Hz, J_2 = 0.5 Hz, 1H, indole C−*H*). $^{13}C\{^1H\}$ NMR (125 MHz, CD_2Cl_2): δ/ppm 151.53 (*s*, indole *C*), 150.78 (*s*, CH═N), 137.99 (*s*, indole *C*), 136.14 (*s*, indole *C*), 129.82 (*s*, *m*-aryl), 128.78 (*s*, *ipso*-aryl), 126.76 (*s*, indole *C*−H), 125.61 (*s*, *p*-aryl), 122.45 (*s*, indole *C*−H), 121.53 (*s*, *o*-aryl), 120.91 (*s*, indole *C*−H), 112.11 (*s*, indole *C*−H), 110.47 (*s*, indole *C*−H). Anal. Calcd (%) for $C_{15}H_{12}N_2$: C, 81.79; H, 5.49; N, 12.72. Found: C, 80.94; H, 5.56; N, 12.52.

Deprotonation of [N,O] and [N,N] Ligand Precursors. *K-(2PyO).* In the glovebox, a CH_2Cl_2 solution (∼10 mL) of **2PyO-H** (0.1 g, 1.05 mmol) was added to a vial containing KO^{t}Bu (0.1178 g, 1.05 mmol), and the mixture was stirred overnight. The slurry produced was then filtered through a frit charged with Celite, and the filtrate was evaporated to dryness under vacuum. A white oily residue remained which was recrystallized from a cold (−35 °C) mixture of THF/diethyl ether (1:1% v/v), filtered, and dried. The yield of **K(2PyO)** was 0.1009 g (0.75 mmol, 71.4%) of gray-white solid. λ_{max} (CH_2Cl_2, 298 K) = 285 nm (ε = 12800 M^{-1} cm^{-1}).

K(2PyN). The compound was prepared following the procedure for **K(2PyO)**, using **2PyN-H** (0.5 g, 3 mmol) and KO^{t}Bu (0.3360 g, 3 mmol). The product was recrystallized from a cold (−35 °C) mixture of CH_2Cl_2/*n*-hexanes (1:1% v/v) to give a pale brown solid. The yield of **K(2PyN)** was 0.5626 g (2.7 mmol, 93.1%). ^1H NMR (400 MHz, CD_2Cl_2): δ/ppm 8.28 (*s*, 1H, C*H*=N), 7.38 (*t*, J_{HH} = 8.8 Hz, 2H, *o*-aryl), 7.22−7.17 (*m*, 3H, *m*-, *p*-aryl), 6.94 (pseudo *t*, J_{HH} = 1 Hz, 1H, pyrrole C−*H*), 6.69 (*dd*, J_1 = 3.6 Hz, J_2 = 1.6 Hz, 1H, pyrrole C−*H*), 6.29 (*dd*, J_1 = 3.6 Hz, J_2 = 2.4 Hz, 1H, pyrrole C−*H*). $^{13}C\{^1H\}$ NMR (100 MHz, CD_2Cl_2): δ/ppm 151.79 (*s*, *ipso*-aryl), 149.71 (*s*, *C*H═N), 130.87 (*s*, pyrrole *C*), 129.15 (*s*, *m*-aryl), 125.36 (*s*, *p*-aryl), 123.01 (*s*, pyrrole *C*−H), 120.84 (*s*, *o*-aryl), 116.37 (*s*, pyrrole *C*−H), 110.3 (*s*, pyrrole *C*−H). λ_{max} (CH_2Cl_2, 298 K) = 326 nm (ε = 26650 M^{-1} cm^{-1}). λ_{ex} (CH_2Cl_2, 298 K) = 359 nm. λ_{em} (CH_2Cl_2, 298 K) = 404 nm. Φ_{em} = 0.09%.

K(2IndO). The compound was prepared and recrystallized following the procedures for **K(2PyN)**, using **2IndO-H** (0.1006 g, 0.69 mmol) and KO^{t}Bu (0.076 g, 0.68 mmol). The yield of **K(2IndO)** was 0.126 g (0.68 mmol, 98.5%) of a dark red solid. λ_{max} (CH_2Cl_2, 298 K) = 276 nm (ε = 9225 M^{-1} cm^{-1}), 306 (ε = 8000 M^{-1} cm^{-1}), 321 (ε = 6175 M^{-1} cm^{-1}), 336 (ε = 5850 M^{-1} cm^{-1}), 370 (ε = 1650 M^{-1} cm^{-1}), 408 (ε = 850 M^{-1} cm^{-1}). λ_{ex} (CH_2Cl_2, 298 K) = 336 nm. λ_{em} (CH_2Cl_2, 298 K) = 421 nm. Φ_{em} = 28%.

K(2IndN). The compound was prepared and recrystallized following the procedure for **K(2PyN)**, using **2IndN-H** (0.0502 g, 0.23 mmol) and KO^{t}Bu (0.0262 g, 0.23 mmol). The yield of **K(2IndN)** was 0.0138 g (0.053 mmol, 23%) of a brown solid. λ_{max} (CH_2Cl_2, 298 K) = 338 nm (ε = 34000 M^{-1} cm^{-1}). λ_{ex} (CH_2Cl_2, 298 K) = 365 nm. λ_{em} (CH_2Cl_2, 298 K) = 423 nm. Φ_{em} = 0.19%.

Preparation of Copper(I) Compounds. *[Cu(2PyN)(Ph$_3$P)$_2$] (**1**).* In the glovebox, a pale yellow-orange solution of **K(2PyN)** (0.031 g, 0.15 mmol) in CH_2Cl_2 (15 mL) was added to $[Cu(NO_3)(Ph_3P)_2]$ (0.100 g, 0.15 mmol). The solution turned bright orange and then turbid as a result of the precipitation of KNO_3. The mixture was stirred for 12 h, filtered through Celite, and evaporated to dryness under a vacuum. A light yellow solid residue (0.0912 g) was obtained, which was recrystallized from cold (−35 °C) CH_2Cl_2 and hexanes to give orange crystals. The yield of **1** was 0.0895 g (0.12 mmol, 80%). ^1H NMR (500 MHz, CD_2Cl_2): δ/ppm 8.31 (*s*, 1H, C*H*=N), 7.42−7.39 (*m*, 5H, phenyl protons of 2PyN), 7.28−7.24 (*m*, 30H, phenyl protons of PPh_3), 7.10 (*m*, 1H, pyrrole C−*H*), 6.94 (*m*, 1H, pyrrole C−*H*), 6.34 (*dd*, J_1 = 3.5 Hz, J_2 = 1.5 Hz, 1H, pyrrole C−*H*). $^{13}C\{^1H\}$ NMR (125 MHz, CD_2Cl_2): δ/ppm 153.99 (*s*, *C*H═N), 152.1 (*s*, pyrrole *C*), 141.14 (*s*, *ipso*-aryl of 2PyN), 137.46 (*s*, *p*-aryl of 2PyN), 134.14 (*d*, $^2J_{C-P}$ = 15.5 Hz, *o*-aryl of PPh_3), 133.85 (*s*, *o*-aryl of 2PyN), 132.45 (*s*, *m*, *ipso*-aryl of PPh_3), 130.23 (*br s*, *p*-aryl of PPh_3), 129.11 (*d*, $^3J_{C-P}$ = 8.7 Hz, *m*-aryl of PPh_3), 124.04 (*s*, pyrrole *C*−H), 122.19 (*s*, *m*-aryl of 2PyN), 118.2 (*s*, pyrrole *C*−H), 112.51 (*s*, pyrrole *C*−H). $^{31}P\{^1H\}$ NMR (202 MHz, CD_2Cl_2): δ/ppm −0.96 (*br s*). Anal. Calcd (%) for $[(Ph_3P)_2$-$Cu(2PyN)]\cdot CH_2Cl_2$ = $C_{48}H_{41}Cl_2CuN_2P_2$: C, 68.45; H, 4.91; N, 3.33. Found: C, 68.29; H, 4.79; N, 3.12.

*[Cu(2PyN)(dppb)] (**2**).* CuCl (0.1003 g, 1 mmol) was dissolved in MeCN (2 mL), and dppb (0.4466 g, 1 mmol) in CH_2Cl_2 (∼10 mL) solution was added to it. An immediate color change from pale green to yellow took place, followed by precipitation of a green yellow solid attributed to $[(dppb)Cu(\mu\text{-}Cl)]_2$. The mixture was stirred for 1 h, after which time **K(2PyN)** (0.2085 g, 1 mmol) was also added. A bright yellow solution was obtained that gradually darkened to a brown slurry. The mixture was stirred for 12 h and then filtered through a frit charged with Celite. Evaporation of the solvent in vacuo yielded an orange solid residue (0.5725 g) which was recrystallized from cold (−35 °C) CH_2Cl_2 and hexanes to give yellow-brown crystals. The yield of **2** was 0.5706 g (0.84 mmol, 84%). ^1H NMR (500 MHz, CD_2Cl_2): δ/ppm 8.40 (pseudo *d*, J_1 = 0.5 Hz, 1H, C*H*=N), 7.60−7.54 (*m*, 4H, *o*-, *m*-aryl of 2PyN), 7.38−7.25 (*m*, 21H, *p*-aryl of 2PyN and phenyl protons of $ArPPh_2$), 6.99−6.96 (*m*, 3H, pyrrole C−*H* and backbone C-*H*), 6.93−6.90 (*m*, 3H, pyrrole C−*H* and backbone C-*H*), 6.45 (*dd*, J_1 = 3.5 Hz, J_2 = 1.5 Hz, 1H, pyrrole C−*H*). $^{13}C\{^1H\}$ NMR (125 MHz, CD_2Cl_2): δ/ppm 153.53 (*s*, CH═N), 151.27 (*s*, pyrrole *C*), 143.48 (*t*, $^1J_{C-P}$ = 33 Hz, backbone *C*−P), 141.29 (*s*, *ipso*-aryl of 2PyN), 137.6 (*s*, *p*-aryl of 2PyN), 134.76 (*t*, $^2J_{C-P}$ = 4 Hz, *o*-aryl of $ArPPh_2$), 134.53 (*t*, $^1J_{C-P}$ = 15.5 Hz, *ipso*-aryl of $ArPPh_2$), 133.76 (*br s*, backbone *C*−H), 130.79 (*s*, *m*-aryl of 2PyN), 129.85 (*br s*, backbone *C*−H), 129.12 (*s*, *p*-aryl of $ArPPh_2$), 128.96 (*t*, $^3J_{C-P}$ = 4.5 Hz, *m*-aryl of $ArPPh_2$), 124.18 (*s*, pyrrole *C*−H), 122.09 (*s*, *o*-aryl of 2PyN), 117.74 (*s*, pyrrole *C*−H), 112.84 (*s*, pyrrole *C*−H). $^{31}P\{^1H\}$ NMR (202 MHz, CD_2Cl_2): δ/ppm −8.43 (*br s*). Anal. Calcd (%) for $[(dppb)Cu(2PyN)]\cdot {}^1/_2(CH_2Cl_2)$ = $C_{42}H_{34}ClCuN_2P_2$: C, 69.32; H, 4.71; N, 3.85. Found: C, 68.50; H, 4.52; N, 3.80.

*[Cu(2PyN)(DPEPHOS)] (**3**).* The compound was prepared following the procedure for **2**, using CuCl (0.5 g, 0.5 mmol), DPEPHOS (0.2693 g, 0.5 mmol), and **K(2PyN)** (0.1047 g, 0.5 mmol). A crude yellow solid (0.3378 g) was obtained from this reaction. Recrystallization from cold (−35 °C) CH_2Cl_2 and *n*-hexanes resulted in formation of yellow-brown crystals. The yield of **3** was 0.2757 g (0.36 mmol, 72%). ^1H NMR (500 MHz, CD_2Cl_2): δ/ppm 8.40 (pseudo *d*, J_1 = 1 Hz, 1H, C*H*=N), 7.4−7.19 (*m*, 25H, *p*-aryl of 2PyN, backbone C−*H* and phenyl protons of $ArPPh_2$), 7.1 (*d*, *J* = 7 Hz, 2H, *o*-aryl of 2PyN), 7.05 (*d*, *J* = 7 Hz, 2H, *m*-aryl of 2PyN), 6.96 (*dt*, J_1 = 13.5 Hz, J_2 = 7.5 Hz, 4H, backbone C−*H*), 6.89 (pseudo *t*, *J* = 7.5 Hz, 1H, pyrrole C−*H*), 6.85 (*d*, *J* = 3 Hz, 1H, pyrrole C−*H*), 6.73−6.7 (*m*, 2H, backbone C−*H*), 6.28 (*dd*, J_1 = 3.5 Hz, J_2 = 1 Hz, 1H, pyrrole C−*H*). $^{13}C\{^1H\}$ NMR (125 MHz, CD_2Cl_2): δ/ppm 159.1 (*t*, $^2J_{C-P}$ = 6.4 Hz, backbone *C*−O), 153.1 (*s*, *C*H═N), 151.42 (*s*, pyrrole *C*), 141.16 (*s*, *ipso*-aryl of 2PyN), 137.3 (*s*, *p*-aryl of 2PyN), 134.81 (*s*, backbone *C*−H), 134.24 (*t*, $^2J_{C-P}$ = 7.6 Hz, *o*-aryl of $ArPPh_2$), 133.62 (*t*, $^1J_{C-P}$ = 14.8 Hz, backbone *C*−P), 131.33 (*s*, *m*-aryl of 2PyN), 129.7 (*s*, backbone *C*−H), 128.85 (*s*, *p*-aryl of $ArPPh_2$), 128.62 (*t*, $^3J_{C-P}$ = 4.5 Hz, *m*-aryl of $ArPPh_2$), 126.54 (*t*, $^1J_{C-P}$ = 11.4 Hz, *ipso*-aryl of $ArPPh_2$), 124.73 (*s*, backbone *C*−H), 123.75 (*s*, pyrrole *C*−H), 122.12 (*s*, *o*-aryl of 2PyN), 120.7 (*s*, backbone *C*−H), 117.55 (*s*, pyrrole *C*−H), 112.2 (*s*, pyrrole *C*−H). $^{31}P\{^1H\}$ NMR (202 MHz, CD_2Cl_2): δ/ppm −15.22 (*br s*), −16.6 (*br s*). Anal. Calcd (%) for $[(DPEPHOS)Cu(2PyN)]\cdot 2(CH_2Cl_2)$ = $C_{49}H_{41}Cl_4CuN_2OP_2$: C, 62.53; H, 4.39; N, 2.98. Found: C, 63.24; H, 4.31; N, 3.11.

*[Cu(2PyN)(XANTPHOS)] (**4**).* The compound was prepared following the procedure for **2**, using CuCl (0.0505 g, 0.5 mmol), XANTPHOS (0.2896 g, 0.5 mmol), and K(2PyN) (0.1048 g, 0.5 mmol), which resulted in formation of a yellow solid (0.3479 g). Slow diffusion of a CH_2Cl_2 solution of **4** into hexanes (20 mL) at −30 °C yielded two crops of purified product. The yield of **4** was 0.2966 g (0.36 mmol, 70.6%). ^1H NMR (400 MHz, CD_2Cl_2): δ/ppm 8.43 (*s*, 1H, C*H*=N),

dx.doi.org/10.1021/ic2007588 |*Inorg. Chem.* 2011, 50, 7172–7188

7.56 (*dd*, J_1 = 7.8 Hz, J_2 = 1.4 Hz, 2H, backbone C−*H*), 7.28−7.08 (*m*, 21H, phenyl protons of $ArPPh_2$), 7.02 (partially resolved *t*, *J* = 7.6 Hz, 2H, backbone C−*H*), 6.87−6.85 (*m*, 2H, *o*-aryl of 2PyN), 6.84−6.78 (*m*, 2H, *m*-aryl of 2PyN), 6.77−6.74 (*m*, 2H, pyrrole C−*H*), 6.44−6.39 (*m*, 2H, backbone C−*H*), 6.19 (*dd*, J_1 = 3.4 Hz, J_2 = 1.4 Hz, 1H, pyrrole C−*H*), 1.85 (*s*, 3H, Me), 1.63 (*s*, 3H, Me). $^{13}C\{^1H\}$ NMR (100 MHz, CD_2Cl_2): δ/ppm 155.96 (*t*, $^2J_{C-P}$ = 5 Hz, backbone *C*−O), 152.45 (*s*, *C*H═N), 150.98 (*s*, pyrrole *C*), 141.33 (*s*, *ipso*-aryl of 2PyN), 137.19 (*s*, *p*-aryl of 2PyN), 134.5 (*t*, $^2J_{C-P}$ = 8.5 Hz, *o*-aryl of $ArPPh_2$), 134.37−134.21 (*m*, backbone *C*−P), 133.35 (*t*, $^2J_{C-P}$ = 8 Hz, *o*-aryl of $ArPPh_2$), 131.41 (*s*, *m*-aryl of 2PyN), 130.41 (*s*, backbone *C*−C-$(Me)_2$), 129.89 (*s*, backbone CH−CP), 129.43 (*s*, backbone *C*H−CP), 128.89 (*s*, *p*-aryl of $ArPPh_2$), 128.76 (*t*, $^3J_{C-P}$ = 5 Hz, *m*-aryl of $ArPPh_2$), 128.64 (*t*, $^3J_{C-P}$ = 5 Hz, *m*-aryl of $ArPPh_2$), 126.41 (*s*, backbone *C*−H), 124.79 (*s*, backbone *C*−H), 123.73 (*s*, pyrrole *C*−H), 122.63 (*t*, $^1J_{C-P}$ = 13 Hz, *ipso*-aryl of $ArPPh_2$), 121.45 (*s*, *o*-aryl of 2PyN), 117.97 (*s*, pyrrole *C*−H), 112.34 (*s*, pyrrole *C*−H), 36.6 (*s*, $C(Me)_2$), 30.24 (*s*, Me), 26.33 (*s*, Me). $^{31}P\{^1H\}$ NMR (162 MHz, CD_2Cl_2): δ/ppm −14.5 (*br s*), −17.7 (*br s*). Anal. Calcd (%) for [(XANTPHOS)Cu(2PyN)] = $C_{50}H_{41}CuN_2OP_2$: C, 74.02; H, 5.09; N, 3.45. Found: C, 72.99; H, 4.79; N, 3.48.

[Cu(2PyO)(DPEPHOS)] (***5***). Similarly to the previous procedures, the compound was prepared from CuCl (0.0501 g, 0.5 mmol) and DPEPHOS (0.270 g, 0.5 mmol) in MeCN solution. **K(2PyO)** was prepared fresh from **2PyO-H** (0.0471 g, 0.5 mmol) and KO^{t}Bu (0.0563 g, 0.5 mmol) and then added to the copper(I) slurry. A yellow-brown solution was produced, accompanied by extensive precipitation of KCl. The mixture was stirred for 12 h. Standard workup and recrystallization from CH_2Cl_2 and hexanes yielded pale yellow crystals. The yield of **5** was 0.1608 g (0.23 mmol, 46%). An alternative preparation of this compound in refluxing ethanol/CH_2Cl_2 (1:1% v/v, ∼40 mL) for 12 h, using the same amounts of starting materials, resulted in extensive formation of the large pale-yellow single crystals of **5** (40% yield). ^1H NMR (400 MHz, CD_2Cl_2): δ/ppm 9.02 (pseudo *d*, J_1 = 1 Hz, 1H, C*H*=O), 7.35−7.23 (*m*, 21H, *o*-, *m*-, and *p*-aryl of $ArPPh_2$ and pyrrole C−*H*), 7.19 (partially resolved *td*, J_1 = 2 Hz, J_1 = 0.4 Hz, 2H, backbone C−*H*), 6.97 (*dd*, J_1 = 0.9 Hz, J_1 = 0.2 Hz, 1H, pyrrole C−*H*), 6.92−6.87 (*m*, 4H, backbone C−*H*), 6.64 (*m*, 2H, backbone C−*H*), 6.36 (*dd*, J_1 = 0.9 Hz, J_2 = 0.3 Hz, 1H, pyrrole C−*H*). $^{13}C\{^1H\}$ NMR (100 MHz, CD_2Cl_2): δ/ppm 179.49 (*s*, *C*H═O), 158.58 (*t*, $^2J_{C-P}$ = 6 Hz, backbone *C*−O), 143.75 (*s*, pyrrole *C*), 139 (*s*, pyrrole *C*−H), 134.67 (*s*, backbone *C*−H), 134.47 (*t*, $^2J_{C-P}$ = 9 Hz, *o*-aryl of $ArPPh_2$), 132.88 (*t*, $^1J_{C-P}$ = 16 Hz, backbone *C*−P), 131.42 (*s*, backbone *C*−H), 130.1 (*s*, *p*-aryl of $ArPPh_2$), 128.91 (*t*, $^3J_{C-P}$ = 4.5 Hz, *m*-aryl of $ArPPh_2$), 125.98 (*t*, $^1J_{C-P}$ = 10 Hz, *ipso*-aryl of $ArPPh_2$), 124.80 (*s*, backbone *C*−H), 121.23 (*s*, pyrrole *C*−H), 120.54 (*s*, backbone *C*−H), 113.43 (*s*, pyrrole *C*−H). $^{31}P\{^1H\}$ NMR (162 MHz, CD_2Cl_2): δ/ppm −17.48 (*br s*). Anal. Calcd (%) for [(DPEPHOS)Cu(2PyO)] 1.5(CH_2Cl_2) = $C_{43}H_{35}Cl_3CuNO_2P_2$: C, 62.25; H, 4.25; N, 1.69. Found: C, 62.06; H, 4.95; N, 1.95.

[Cu(2PyO)(XANTPHOS)] (***6***). The compound was prepared following the procedure indicated for **5**, using CuCl (0.05 g, 0.5 mmol), XANTPHOS (0.2903 g, 0.5 mmol), and **K(2PyO)**, prepared in situ from **2PyO-H** (0.0475 g, 0.5 mmol) and KO^{t}Bu (0.0566 g, 0.5 mmol) in a mixture of CH_2Cl_2/MeCN (10:1% v/v, ∼10 mL). The latter was refluxed at 80 °C for 24 h. The workup of this mixture and recrystallization from CH_2Cl_2 and hexanes yielded pale yellow crystals. The yield of **6** was 0.2803 g (0.38 mmol, 76%). ^1H NMR (400 MHz, CD_2Cl_2): δ/ppm 9.13 (*s*, 1H, C*H*=O), 7.58 (*dd*, J_1 = 7.6 Hz, J_2 = 1.6 Hz, 2H, backbone C−*H*), 7.28−7.13 (*m*, 21H, *o*-, *m*-, and *p*-aryl of $ArPPh_2$, pyrrole C−*H*), 7.09 (partially resolved *t*, *J* = 7.6 Hz, 2H, backbone C−*H*), 7.02 (*d*, *J* = 7.6 Hz, 1H, pyrrole C−*H*), 6.51 (*m*, 2H, backbone C−*H*), 6.34 (*dd*, J_1 = 3.6 Hz, J_2 = 1.2 Hz, 1H, pyrrole C−*H*), 1.68 (*s*, 6H, Me). $^{13}C\{^1H\}$ NMR (125 MHz, CD_2Cl_2): δ/ppm 179.83 (*s*, *C*H═O), 155.99 (*br*, backbone *C*−O), 143.9 (*s*, pyrrole *C*), 138.89 (*s*, pyrrole *C*−H), 134.46 (*s*, backbone *C*−$C(Me)_2$), 134.19 (*t*, $^2J_{C-P}$ = 6.2 Hz, *o*-aryl of $ArPPh_2$), 133.59 (*t*, $^1J_{C-P}$ = 12.3 Hz, backbone *C*−P), 131.81 (*s*, backbone *C*−H), 129.94 (*s*, *p*-aryl of $ArPPh_2$), 128.86 (*br s*, *m*-aryl of $ArPPh_2$), 126.87 (*s*, backbone *C*−H), 124.98 (*s*, backbone *C*−H), 122.02 (*t*, $^1J_{C-P}$ = 10 Hz, *ipso*-aryl of $ArPPh_2$), 121.44 (*s*, pyrrole *C*−H), 113.43 (*s*, pyrrole *C*−H), 35.26 (*s*, $C(Me)_2$), 32.2 (*s*, Me). $^{31}P\{^1H\}$ NMR (162 MHz, CD_2Cl_2): δ/ppm −16.65 (*br s*). Anal. Calcd (%) for [(XANTPHOS)Cu(2PyO)] = $C_{44}H_{36}CuNO_2P_2$: C, 71.78; H, 4.93; N, 1.90. Found: C, 71.05; H, 5.70; N, 1.43.

[Cu(2IndO)(DPEPHOS)] (***7***). The compound was prepared following the procedure indicated for **5**, using CuCl (0.1007 g, 1 mmol), DPEPHOS (0.539 g, 1 mmol), **2IndO-H** (0.1447 g, 1 mmol), and KO^{t}Bu (0.1121 g, 1 mmol). A green yellow solid (0.7912 g) crashed out after the mixing of the reactants and required several washings with CH_2Cl_2 (5 × 20 mL), to extract and separate it from produced KCl during filtration. Recrystallization from CH_2Cl_2 and hexanes at low temperature (−30 °C) yielded two crops of pure product. The yield of **7** was 0.6538 g (0.79 mmol, 79%) of green yellow crystals. ^1H NMR (500 MHz, CD_2Cl_2): δ/ppm 9.64 (*s*, 1H, C*H*=O), 7.58 (*dd*, J_1 = 7 Hz, J_2 = 1 Hz, 1H, indole C−*H*), 7.55 (*br q*, *J* = 5.5 Hz, 2H, indole C−*H*), 7.46−7.23 (*m*, 22H, *o*-, *m*-, and *p*-aryl of $ArPPh_2$, indole C−*H*), 7.14 (*dd*, J_1 = 8 Hz, J_2 = 1 Hz, 1H, backbone C−*H*), 7.06 (*d*, *J* = 7.5 Hz, 1H, backbone C−*H*), 7.02 (*t*, *J* = 7.5 Hz, 1H, backbone C−*H*), 6.96 (*t*, *J* = 7.5 Hz, 2H, backbone C−*H*), 6.91 (*m*, 2H, backbone C−*H*), 6.74 (*m*, 1H, backbone C−*H*). $^{13}C\{^1H\}$ NMR (125 MHz, CD_2Cl_2): δ/ppm 186.36 (*s*, *C*H═O), 159.03 (*t*, $^2J_{C-P}$ = 6.3 Hz, backbone *C*−O), 158.36 (*t*, $^2J_{C-P}$ = 6.3 Hz, backbone *C*−O), 148.53 (*s*, indole *C*−CHO), 146.96 (*s*, indole *C*), 134.77 (*t*, $^2J_{C-P}$ = 7.5 Hz, backbone *C*−H), 134.64 (*t*, $^2J_{C-P}$ = 7.5 Hz, backbone *C*−H), 134.49 (*t*, $^2J_{C-P}$ = 7.5 Hz, *o*-aryl of $ArPPh_2$), 132.75 (*t*, $^1J_{C-P}$ = 16.1 Hz, backbone *C*−P), 132.01 (*s*, backbone *C*−H), 131.64 (*s*, backbone *C*−H), 131.33 (*s*, indole *C*), 130.75 (*s*, indole *C*−H), 130.18 (*br s*, *p*-aryl of $ArPPh_2$), 129.29 (pseudo *t*, *J* = 5 Hz, *ipso*-aryl of $ArPPh_2$), 128.98 (*t*, $^3J_{C-P}$ = 4.5 Hz, *m*-aryl of $ArPPh_2$), 125.96 (*t*, $^1J_{C-P}$ = 12.6 Hz, backbone *C*−P), 125.19 (*s*, backbone *C*−H), 124.99 (*s*, backbone *C*−H), 123.25 (*d*, $^1J_{C-P}$ = 16.6 Hz, indole *C*−H, endo), 120.72 (*s*, backbone *C*−H), 120.37 (*s*, backbone *C*−H), 119.64 (*s*, indole *C*−H), 118.4 (*s*, indole *C*−H), 112.26 (*s*, indole *C*−H). $^{31}P\{^1H\}$ NMR (162 MHz, CD_2Cl_2): δ/ppm −17.52 (*br s*), −19.37 (*br s*). Anal. Calcd (%) for [(DPEPHOS)Cu(2IndO)] 1.5(CH_2Cl_2) = $C_{47}H_{37}Cl_3CuNO_2P_2$: C, 64.17; H, 4.24; N, 1.59. Found: C, 63.89; H, 4.08; N, 1.62.

[Cu(2IndN)(DPEPHOS)] (***8***). The compound was prepared following the procedure indicated for **5**, using CuCl (0.0999 g, 1 mmol), DPEPHOS (0.5398 g, 1 mmol), **2IndN-H** (0.2209 g, 1 mmol), and KO^{t}Bu (0.1130 g, 1 mmol). As with **7**, a yellow solid (0.7513 g) crashed out from solution and several washings with CH_2Cl_2 (3 × 20 mL) were required to filter it through a frit in the first stage of the workup. Recrystallization from CH_2Cl_2 and hexanes at low temperature (−30 °C) also yielded two crops of pure product. The yield of **8** was 0.7589 g (0.92 mmol, 92%) of yellow-brown crystals. ^1H NMR (500 MHz, CD_2Cl_2): δ/ppm 8.43 (*s*, 1H, C*H*=N), 7.65−7.63 (*m*, 1H, indole C−*H*), 7.54 (*br q*, *J* = 5.5 Hz, 1H, indole C−*H*), 7.46−7.4 (*m*, 2H, indole C−*H*), 7.37−7.27 (*m*, 5H, *o*-, *m*-, and *p*-aryl of IndN), 7.25 (*ddd*, J_1 = 8 Hz, J_2 = 1.5 Hz, 1H, indole C−*H*), 7.23−7.07 (*m*, 20H, *o*-, *m*-, and *p*-aryl of $ArPPh_2$), 7.03 (*br d*, J_1 = 7.5 Hz, 2H, backbone C−*H*), 6.95 (*t*, *J* = 7.5 Hz, 2H, backbone C−*H*), 6.84−6.77 (*m*, 4H, backbone C−*H*), 6.74 (*m*, 2H, backbone C−*H*). $^{13}C\{^1H\}$ NMR (125 MHz, CD_2Cl_2): δ/ppm 159.2 (*t*, $^2J_{C-P}$ = 6.4 Hz, backbone *C*−O), 157.91 (*s*, CH═N), 152.1 (*s*, indole *C*−CH=N), 148.63 (*s*, indole *C*), 146.03 (*s*, indole *C*), 134.31 (*s*, backbone *C*−H), 134.31 (*br s*, *o*-aryl of $ArPPh_2$), 133.43 (*t*, $^1J_{C-P}$ = 14.8 Hz, backbone *C*−P), 132.26 (*s*, *ipso*-aryl of 2IndN), 131.42 (*s*, backbone *C*−H), 129.72 (*br s*, *p*-aryl of $ArPPh_2$), 129.24 (pseudo *t*, *J* = 5 Hz, *ipso*-aryl of $ArPPh_2$), 129.08 (*s*, *m*-aryl of 2IndN), 128.68 (pseudo *t*, *J* = 4.4 Hz, *m*-aryl of $ArPPh_2$), 126.78 (*t*, $^1J_{C-P}$ = 14.8 Hz,

dx.doi.org/10.1021/ic2007588 |*Inorg. Chem.* 2011, 50, 7172–7188

backbone *C*−P), 125.18 (*s*, *p*-aryl of 2IndN), 124.78 (*s*, backbone *C*−H), 122.41 (*s*, *o*-aryl of 2IndN), 121.7 (*s*, indole *C*−H), 121.33 (*s*, indole *C*−H), 120.81 (*s*, backbone *C*−H), 118.47 (*s*, indole *C*−H), 117.07 (*s*, indole *C*−H), 107.91 (*s*, indole *C*−H). $^{31}P\{^1H\}$ NMR (202 MHz, CD_2Cl_2): δ/ppm −15.17 (*br s*), −19.47 (*br s*). Anal. Calcd (%) for $[(DPEPHOS)Cu(2IndN)]\cdot{}^1/_2(CH_2Cl_2)$ = $C_{52}H_{40}ClCuN_2OP_2$: C, 71.8; H, 4.64; N, 3.22. Found: C, 71.11; H, 4.87; N, 3.03.

X-ray Structural Determinations. *Data Collections.* Crystals were placed in separate runs onto the tip of a 0.1 mm diameter glass capillary tube or fiber and mounted on a Bruker SMART APEX II CCD Platform diffractometer for a data collection at 100.0(1) K.[19] A preliminary set of cell constants and an orientation matrix were calculated for each crystal from reflections harvested from three orthogonal wedges of reciprocal space. The full data collections were carried out at a detector distance of 4 cm using Mo Kα radiation (graphite monochromator) with the following frame times: **2PyN-H**, 5 s; **1**, 60 s; **2**, 45 s; **3**, 90 s; **5**, 5 s; **6**, 20 s; **7**, 90 s; **8**, 45 s; **9**, 45 s. Randomly oriented regions of reciprocal space were surveyed: (i) **2PyN-H**, **1**, **2**, **5**, **6**, and **8**, four major sections of frames were collected with 0.50° steps in ω at four different φ settings and a detector position of −38° in 2θ. (ii) Compound **3**, four major sections with 0.75° steps in ω at four different φ settings and a detector position of −38° in 2θ. (iii) Compound **7**, three major sections of frames with 0.75° steps in ω at three different φ settings and a detector position of −38° in 2θ. (iv) Compound **9**, three major sections of frames with 0.50° steps in ω at three different φ settings and a detector position of −38° in 2θ. The intensity data were corrected for absorption.[20] The final cell constants were calculated from the *xyz* centroids resulting from approximately 4000 strong reflections from the actual data collection after integration.[21] Tables 4and 5 in the main text summarize crystal data and refinement information for compounds **1**−**8**. Table S-1 in the Supporting Information summarizes the data for compound **9**.

Structure Solutions and Refinements. All of the structures were solved using SIR97[22] and refined using SHELXL-97.[23] Space groups for compounds **2PyN-H** (*Pbca*), **2** ($P2_1/c$), **6** ($P4_2/n$), **7** ($P2_1/n$), and **9** ($C2/c$) were determined on the basis of systematic absences. In the case of compounds **1**, **3**, **5**, and **8**, the space group $P\bar{1}$ was determined on the basis of the intensity statistics alone. A direct-methods solution was calculated for each system, which provided most non-hydrogen atoms from the E-map. Full-matrix least-squares (on F^2) /difference Fourier cycles were performed, which located the remaining non-hydrogen atoms. All non-hydrogen atoms were refined with anisotropic displacement parameters. All hydrogen atoms were placed in ideal positions and refined as riding atoms with relative isotropic displacement parameters except for the structure of **2PyN**, for which the hydrogen atoms were found from the difference Fourier map and refined independently from their bonded heavier atoms with individual isotropic displacement parameters. A summary of the final full matrix least-squares refinements is listed as follows: **2PyN**, converged to $R1 = 0.0502$ (F^2, $I > 2\sigma(I)$) and $wR2 = 0.1499$ (F^2, all data); **1** converged to $R1 = 0.0563$ (F^2, $I > 2\sigma(I)$) and $wR2 = 0.1407$ (F^2, all data); **2** converged to $R1 = 0.0541$ (F^2, $I > 2\sigma(I)$) and $wR2 = 0.1479$ (F^2, all data); **3** converged to $R1 = 0.0613$ (F^2, $I > 2\sigma(I)$) and $wR2 = 0.1654$ (F^2, all data); **5** converged to $R1 = 0.0390$ (F^2, $I > 2\sigma(I)$) and $wR2 = 0.1050$ (F^2, all data); **6** converged to $R1 = 0.0552$ (F^2, $I > 2\sigma(I)$) and $wR2 = 0.1660$ (F^2, all data); **7** converged to $R1 = 0.0791$ (F^2, $I > 2\sigma(I)$) and $wR2 = 0.2553$ (F^2, all data); **8** converged to $R1 = 0.0446$ (F^2, $I > 2\sigma(I)$) and $wR2 = 0.1209$ (F^2, all data); **9** converged to $R1 = 0.0571$ (F^2, $I > 2\sigma(I)$) and $wR2 = 0.1327$ (F^2, all data). For compounds **2** and **3**, two independent molecules cocrystallized in the asymmetric unit (Figures S28 and S29 in the Supporting Information). The pyrrole-aldehyde ligand in complex **6** is modeled as disordered over two positions (61:39), each of which is essentially the inversion of the other within the same plane. In the case of **3** and **6**, highly disordered solvent channels in their structures were found. In compound **3**, two independent solvent channels were found parallel to the *a*-axis. One of them contained well-ordered cocrystallized dichloromethane solvent molecules, whereas the second one contained highly disordered solvent. The latter channel appeared to contain both CH_2Cl_2 and *n*-hexane (or perhaps diethyl ether). Figure S30 in the Supporting Information shows a view of the packing with empty channels. In the case of **6**, only highly disordered solvent molecules were found in channels parallel to the *c*-axis (four per unit cell), which could not be modeled. The reflection contributions from the highly disordered solvent in both **3** and **6** were removed using the program PLATON and the function SQUEEZE,[24] which determined there to be 152 electrons in 416 Å^3 and 380 electrons in 1584 Å^3 removed per unit cell for the structures of these two systems, respectively. In either case, because the exact identities of the solvent molecules removed are unknown, these were not included in the molecular formulas or atom lists of **3** and **6**. As a result, all calculated fields that derive from these (e.g., $F(000)$, density, formula weight, etc.) are known to be incorrect.

RESULTS AND DISCUSSION

Syntheses of [N,N] Ligand Precursors. Pyrrole-2-phenylcarbaldimine (**2PyN-H**) and indole-2-phenylcarbaldimine (**2IndN-H**) were prepared on the basis of the method by Grushin and Marshall for the syntheses of pyrrole-aldimines, which consists of the condensation of pyrrole-2-carboxaldehyde (**2PyO-H**) with alkyl- or aryl-amines (aniline) in aqueous media.[18] The choice of employing phenyl substituted ligands was made on the basis of the stability that the phenyl ring confers.[25] To our knowledge **2IndN-H** has not been prepared previously.[11] The condensation reactions were performed by refluxing the precursor aldehyde in the presence of water and aniline for 12 h. The products were obtained in good yields as air-stable dark red solids (eqs 1 and 2).

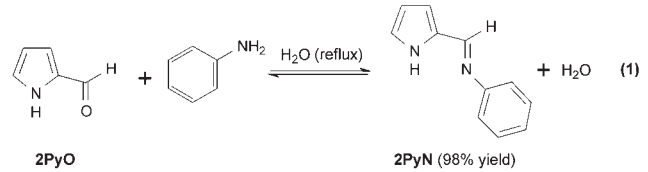

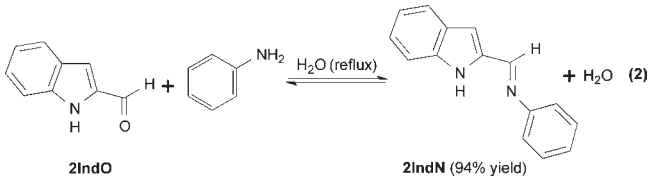

In the ^1H NMR spectra (CD_2Cl_2), the two types of aldimines exhibit a singlet (*s*) characteristic of the C*H*═N moiety at ca. 8.5 ppm that is clearly different from that of the C*H*═O resonance in the starting materials at ca. 9.5 ppm. The same trend is reproduced in the $^{13}C\{^1H\}$ NMR spectra where the *C*H═N signal appears at about 150 ppm, while the *C*H═O peak appears at 179 ppm. The integrated ^1H and the $^{13}C\{^1H\}$ NMR spectra of the two [N,N] ligand precursors are included in the Supporting Information. Crystals of **2PyN-H** suitable for X-ray diffraction (XRD) were obtained from the slow evaporation of a concentrated dichloromethane solution of this compound. The ligand **2PyN-H** crystallizes in the orthorhombic space group *Pbca* with two independent molecules in the asymmetric unit (Figure 1) linked pairwise by intermolecular hydrogen bonding. The molecules are not oriented coplanar to each other, and although dimerization takes place, this does not result in stacking (see

dx.doi.org/10.1021/ic2007588 |*Inorg. Chem.* 2011, 50, 7172–7188

Supporting Information).[26] The complete crystallographic data for **2PyN-H** is summarized in Table 2.

Within each molecule in the asymmetric unit, the N-phenyl ring is twisted out of plane with respect to the pyrrole-aldimine moiety, with torsion angles of 46.59(3)° and 44.13(3)°. The imine C═N distances of 1.287(1)Å and 1.285(1)Å are within the range for this group.[10a,c] The pyrrole-to-aldimine C−C single bond lengths (1.428(1) Å and 1.425(1) Å) are shorter than normal and are consistent with the conjugation of the pyrrole rings with the coplanar C═N bond, a feature that has also been highlighted by Gomes's group with a closely related iminopyrrole.[10b]

Syntheses of Copper(I) Compounds. The carboxaldehyde starting materials and their carbaldimine derivatives were deprotonated in CH_2Cl_2 using potassium *tert*-butoxide (KO^tBu) to provide the potassium salts of the $(N,N)^-$ or $(N,O)^-$ bidentate ligands, $K(L_2)$, where $(L_2)^-$ = $(2PyO)^-$, $(2PyN)^-$, $(2IndO)^-$, or $(2IndN)^-$ (eqs 3 and 4). Neutral heteroleptic copper(I) compounds of the type $[Cu(L_2)(P,P)]$ (P,P = mono- or diphosphine; L_2 = bidentate ligand = $2PyO^-$, $2PyN^-$, $2IndO^-$, or $2IndN^-$), otherwise denoted in this work as [Cu(N,N)(diphosphine)] ((N,N) = 2PyN for compounds **1**−**4** and 2IndN for **8**) or [Cu(N,O)(diphosphine)] ((N,O) = 2PyO for compounds **5**−**6** and 2IndO for **7**), were prepared by salt metathesis using the deprotonated ligands and a neutral source of copper(I). In the preparation of $[Cu(2PyN)(Ph_3P)_2]$ (**1**), $[Cu(NO_3)(Ph_3P)_2]$[14] was used as the starting material. The rest of the $[Cu(L_2)(diphosphine)]$ compounds (**2**−**8**) were synthesized from their diphosphine dimers, $[Cu(\mu\text{-}Cl)(P,P)]_2$ (P,P = dppb, DPEPHOS, XANTPHOS), which were prepared in one step from CuCl and the respective diphosphine in CH_2Cl_2 (Scheme 2).[27]

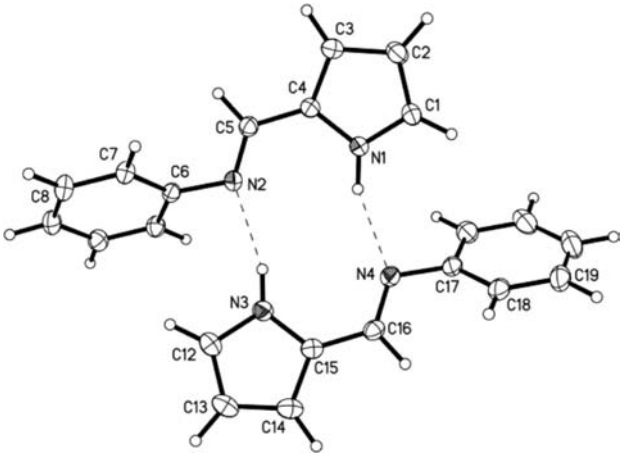

Figure 1. ORTEP representation of the asymmetric unit of **2PyN-H**, showing thermal displacement ellipsoids at the 50% probability level. Hydrogen bond distances (Å): N(1)−H(1N)···N(4) = 2.078(13), N(3)−H(3N)···N(2) = 2.098(14).

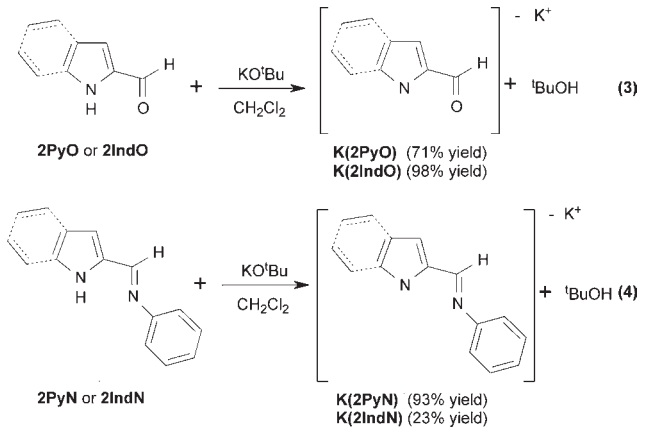

The colors of the product complexes varied from blue-green (**7**) to pale yellow (**5** and **6**) to yellow-brown (**1**−**4** and **8**), depending on the nature of the $(N,N)^-$ or $(N,O)^-$ bidentate ligand. The identities of the complexes were confirmed by multinuclear NMR spectroscopy and by elemental analyses. For compounds **1**−**3** and **5**−**8**, the slow diffusion of concentrated CH_2Cl_2 solutions into hexanes resulted in the formation of single crystals from which the structures in the

Scheme 2

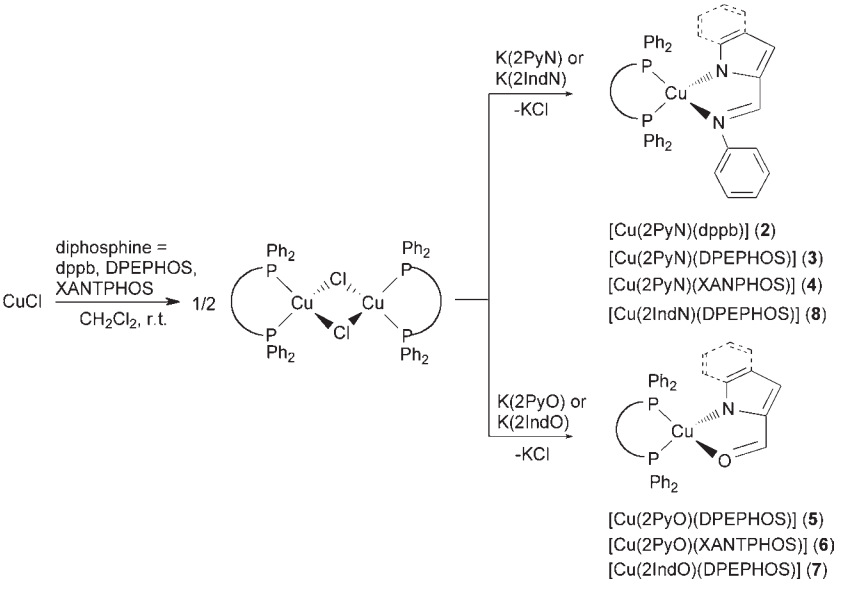

dx.doi.org/10.1021/ic2007588 |*Inorg. Chem.* 2011, 50, 7172–7188

solid state were established by X-ray crystallography. The structure of an additional, unexpected compound, namely {[Cu(XANTPHOS)]$_2$(μ-Cl)(μ-ClCuCl)} (**9**), was also established by the examination of crystals from a batch of [Cu(2PyO)(XANTPHOS)] (**6**), the latter of which represented the majority of the material present in the particular batch. Crystals of **9** were present as trace impurities that were initially thought to be polymorphs of **6**. The finding is interesting because it shows a linear CuCl unit inserted as a bridge onto [Cu(μ-Cl)(XANTPHOS)]$_2$, the precursor of **6**. Additional details along with ORTEP representations of this compound are included in the Supporting Information.

Table 1. Comparison of Distinctive NMR Signals of Free Ligands and Their Corresponding Copper(I) Compounds

	^{1}H NMR		^{13}C{^{1}H} NMR		^{31}P{^{1}H} NMR	
compound	C*H*=O	C*H*=N	C*H*=O	C*H*=N	δ_1	δ_2
2PyO	9.5		179.5			
5	9		179.5		−17.5	
6	9.1		179.8		−16.6	
2PyN		8.5		150.9		
1		8.3		153.9	−0.9	
2		8.4		153.5	−8.4	
3		8.4		153.1	−15.2	−16.6
4		8.4		152.5	−14.5	−17.7
2IndO	9.9		182.7			
7	9.6		186.4		−17.5	−19.4
2IndN		8.6		150.8		
8		8.4		157.9	−15.2	−19.5

The ^{1}H and ^{13}C{^{1}H} NMR spectra of the Cu(I) complexes were compared to those of their free (N,N) or (N,O) ligand precursors, with particular emphasis on the diagnostic resonances of the aldehyde or aldimine moieties (Table 1). In general, only small changes were found for these signals, suggesting that the electronic environments of the ligands remain relatively unperturbed upon coordination. For the [Cu(N,N)(diphosphine)] complexes with pyrrole-aldimine (**1**−**4**) or indole-aldimine (**8**) ligands, a 0.1−0.2 ppm to high field shift was seen for the proton resonance of the coordinated imine. Similarly, the coordination of the ligand is evident in the ^{13}C{^{1}H} NMR spectra as the chemical shift of the C*H*=N peak is increased by approximately 3 ppm for the [Cu(2PyN)(diphosphine)] compounds (**1**−**4**) and by approximately 8 ppm for the indole-aldimine analogue (**8**). Similar analyses apply to the [Cu(N,O)(diphosphine)] ((N,O) = pyrrole-aldehyde (**5**, **6**) or indole-aldehyde (**7**)) compounds, for which the aldehyde proton is more shielded by ca. 0.5 ppm while the carbonyl is more deshielded upon coordination. The C*H*=O resonances of the [Cu(2PyO)(diphosphine)] compounds **5** and **6** in the respective ^{13}C{^{1}H} spectra exhibit a much smaller change (≤0.3 ppm) than the one for C*H*=N of the [Cu(2PyN)(diphosphine)] analogues, **1**−**4** (ca. 2−3 ppm), which is consistent with weaker coordination of the aldehyde relative to the imine. Similar trends are observed when comparing [Cu(2IndO)(DPEPHOS)] (**7**) with [Cu(2IndN)(DPEPHOS)] (**8**).

The presence of coordinated PPh_3 on compound **1**, or coordinated diphosphines for the other copper compounds, was confirmed by ^{31}P{^{1}H} NMR, which typically exhibited

Table 2. Selected Bond Distances (Å) and Angles (deg) for Compounds 1−3 and 5−8 [a]

compound	**2PyN-H**	**1**	**2**[b]	**3**[b]	**5**	**6**	**7**	**8**
bond	distance (Å)							
Cu1−N1		2.042(2)	2.008(1)	2.023(2)	1.995(1)	2.001(3)	1.973(6)	2.015(1)
Cu1−N2		2.115(2)	2.070(1)	2.106(2)				2.144(1)
Cu1−O1					2.279(1)	2.254(3)	2.352(6)	
Cu1−P1		2.2303(6)	2.2385(5)	2.2660(8)	2.2267(4)	2.2475(4)	2.266(2)	2.283(4)
Cu1−P2		2.2363(6)	2.2418(5)	2.2170(8)	2.2784(4)	2.2236(4)	2.228(2)	2.2395(4)
C4−C5	1.428(1)	1.406(3)	1.414(2)	1.415(4)	1.411(2)	1.319(12)	1.43(1)	1.432(2)
N2−C5	1.287(1)	1.291(3)	1.308(2)	1.292(4)				1.293(2)
O1−C5					1.2487(2)	1.289(6)	1.25(1)	
angle				angle (deg)				
N1−Cu1−N2		81.48(7)	82.76(6)	81.9(1)				81.10(5)
N1−Cu1−O1					80.71(4)	80.55(14)	78.2(2)	
P1−Cu1−P2		122.57(2)	87.30(2)	110.25(3)	114.86(1)	115.84(1)	115.84(8)	113.24(1)
N2−C5−C4	123.85(7)	120.1(2)	119.78(14)	119.7(3)				119.2(1)
O1−C5−C4					123.1(1)	123.5(5)	122.3(8)	
dihedral angle				angle (deg)				
P−Cu−P$^{\perp}$N−Cu−N		82.56(2)	86.02(4)	82.73(6)				88.72(3)
P−Cu−P$^{\perp}$O−Cu−N					83.47(3)	87.39(7)	84.9(2)	
ligand tilt				angle (deg)				
{Pyrrole-C(5)−N(2)}$^{\perp}${Ph}	46.59(3)	44.97(8)	30.53(9)	32.4(2)				
{Indole-C(5)−N(2)}$^{\perp}${Ph}								19.85(4)

[a] Selected data for **2PyN-H** is included for additional comparison purposes. [b] Refers to one of the independent molecules cocrystallized in the asymmetric unit (Figures S28 and S29 in the Supporting Information).

dx.doi.org/10.1021/ic2007588 |*Inorg. Chem.* 2011, 50, 7172–7188

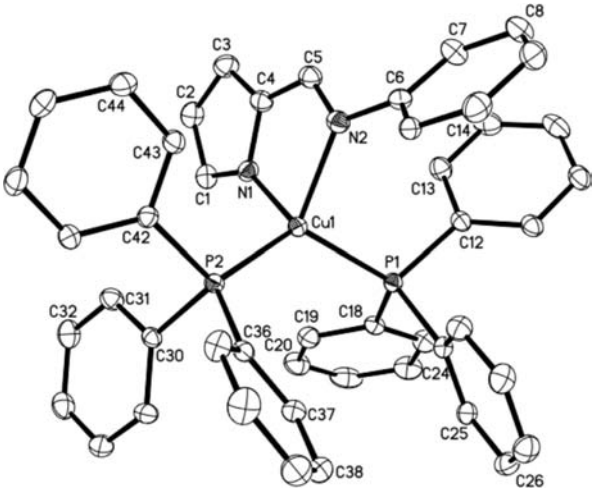

Figure 2. Molecular structure of **1**. Hydrogen atoms have been omitted for clarity.

broad signals. The spectra of [Cu(2PyN)(DPEPHOS)] (**3**), [Cu(2PyN)(XANTPHOS)] (**4**), [Cu(2IndO)(DPEPHOS)] (**7**), and [Cu(2IndN)(DPEPHOS)] (**8**) exhibited two broad peaks of unequal intensity, which were interpreted as resulting from coordination isomers as a result of the arrangement of the (N,N) or (N,O) ligand with respect to the puckered diphosphine ligands (Table 1). Analysis of the solid state structure for compound **6** provides evidence for this assumption. There is a disorder in the (N,O) ligand in which each position is essentially the inverse of the other within the same plane. While the phosphorus atoms within each isomer are equivalent via a mirror plane, they are inequivalent between isomers. The isomers can interconvert by dissociation and recoordination of the anionic ligand or by the twisting of the diphosphine. Although only a single ^{31}P resonance was observed for compound **6**, the presence of such coordination isomers in **3**−**4** and **7**−**8** in solution is possible especially if the additional steric bulk provided by the N-phenyl aldimine or indole rings prevents rapid isomerization via twisting of the diphosphine ligand.

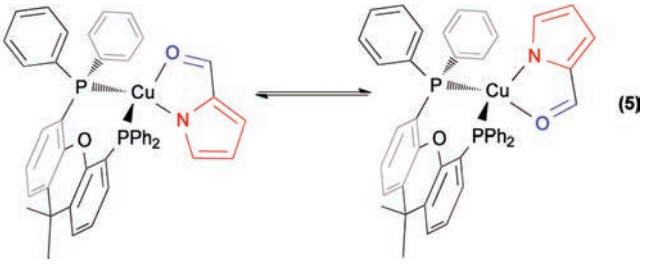

(5)

Because thermal stability and sublimability are critical properties for successful OLED device preparation by vapor deposition, small scale sublimations were attempted for complexes **2**−**4**. Successful sublimation occurred at 230−250 °C under vacuum (ca. 2×10^{-3} Torr) with approximately 40% recovery.

Molecular Structures of Copper(I) Compounds. The structures of compounds **1**−**3** and **5**−**8** were established by the X-ray diffraction of single crystals (Figures 2−8). Table 2 summarizes the relevant bond distances and angles for these compounds, and all other data are available in the Supporting Information in cif format. The complete crystallographic data and structure

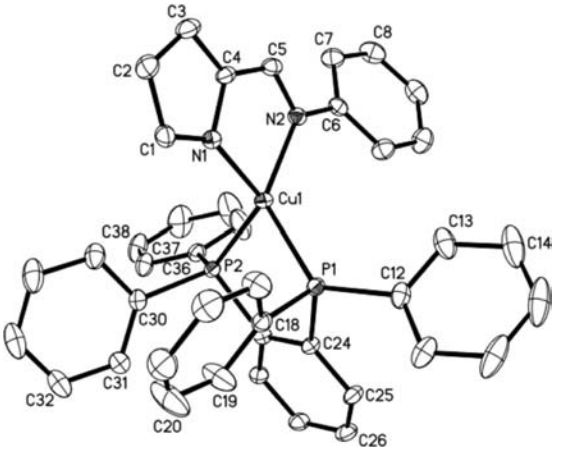

Figure 3. Molecular structure of one independent molecule of **2**. Hydrogen atoms have been omitted for clarity.

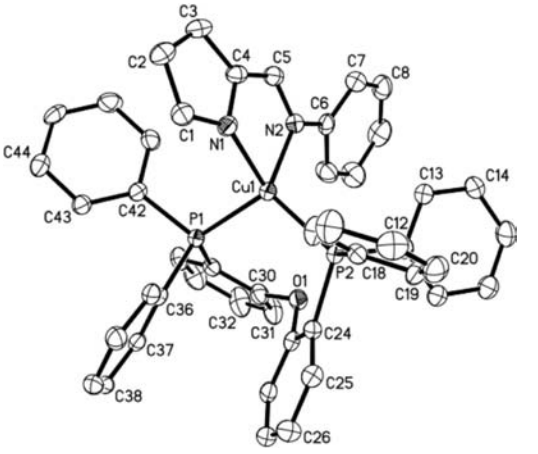

Figure 4. Molecular structure of one independent molecule of **3**. Hydrogen atoms have been omitted for clarity.

refinement details are summarized in Tables 3 and 4. Unless otherwise noted, all structural diagrams containing thermal displacement ellipsoids are drawn at the 50% probability level.

Both the (N,N) and (N,O) bidentate ligands, structures form five-membered chelate rings with copper(I). For the [Cu(N,N)(diphosphine)] series, **1**−**3** and **8**, the pending phenyl substituent is tilted out of plane from the pyrrole- or indole-aldimine unit, with dihedral angles varying from 19.85(4)° in **8** to 46.59(3)° in **1** (Table 2). For **1**−**3**, the comparison of the C4−C5 and N2−C5 bond lengths with the corresponding ones of the ligand precursor, **2PyN-H**, shows that the C−C bond distance is slightly shorter, whereas the C−N bond is longer, in the complexes. The N2−C5−C4 angle of the copper(I) compounds (mean ∼119.86°) is slightly more acute than that of **2PyN-H** (123.85°). In **8**, both C−C and N−C bond distances are slightly elongated compared to the case of the free ligand.

The N−Cu−N bond angles are very similar among the [Cu(N,N)(diphosphine)] compounds, but the P−Cu−P angle varies more so, ranging from 87.296(19)° for **2** to 113.239(14)° in **8**. For the [Cu(N,O)(diphosphine)] complexes, neither the N−Cu−O nor the P−Cu−P bond angles exhibit a great variation. The dihedral angle between the P−Cu−P and N−Cu−N planes for the [Cu(pyrrole-aldimine)(diphosphine)]

dx.doi.org/10.1021/ic2007588 |*Inorg. Chem.* 2011, 50, 7172–7188

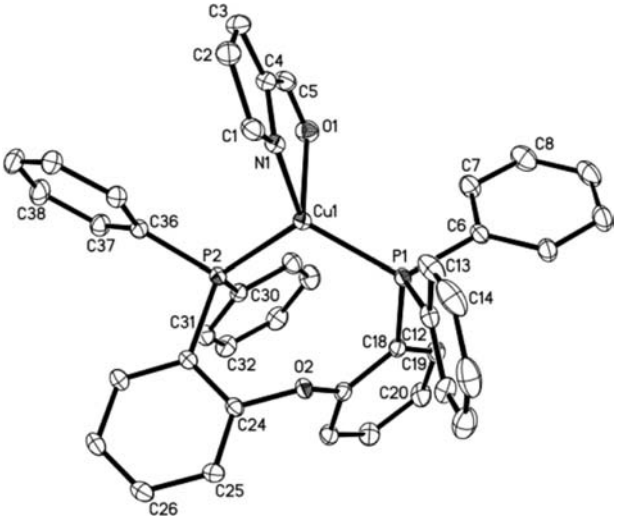

Figure 5. Molecular structure of **5**. Hydrogen atoms have been omitted for clarity.

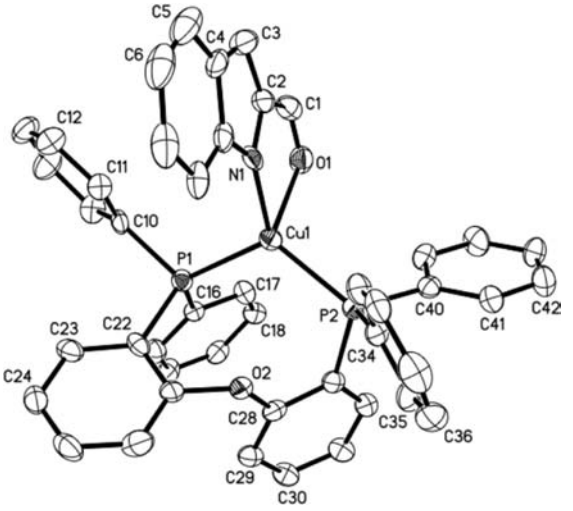

Figure 7. Molecular structure of **7**. Hydrogen atoms have been omitted for clarity.

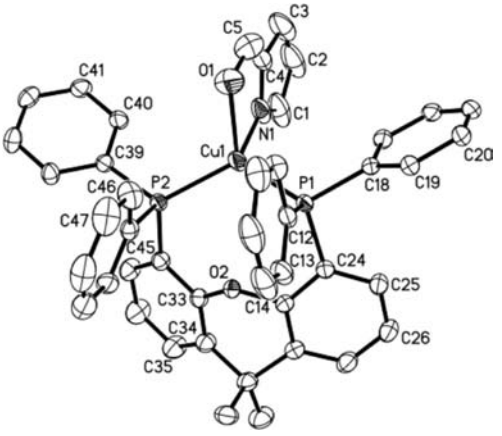

Figure 6. Molecular structure of **6**. Hydrogen atoms have been omitted for clarity.

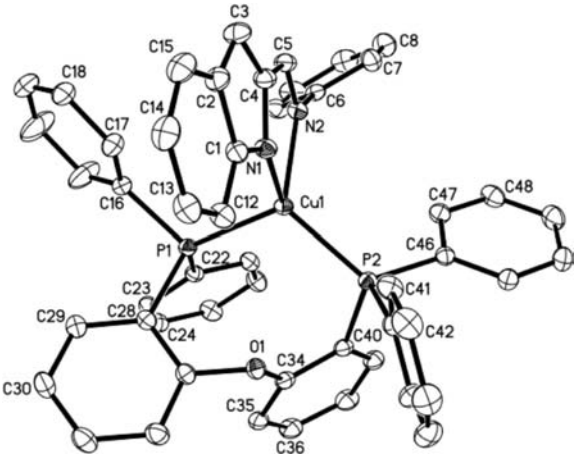

Figure 8. Molecular structure of **8**. Hydrogen atoms have been omitted for clarity.

compounds **1**−**3** (mean ∼83.77°) and the [Cu(indole-aldimine)(diphosphine)] compound (**8**) (88.72°) reveals a distorted tetrahedral geometry around the copper(I) ion for all of the structures and is consistent with previously reported structures of heteroleptic phosphine- or diphosphine-based copper(I) complexes containing (N,N) donors.[6j,k,7] The same observation holds true for the indole-aldehyde complexes **5** and **6** (mean ∼85.43°) and the indole-aldehyde complex **7** (84.93°), even though the aldehyde functional group encounters much less steric congestion than the substituted imine does.

Spectroscopic Properties in Fluid Solution. The absorption and emission spectra of the potassium salts of the deprotonated ligands (Figure S34 in the Supporting Information) and their respective copper(I) compounds (Figures 9−12) were measured in CH_2Cl_2, at room temperature (298 K). All data are summarized in Table 5.

Ligand emission spectra are characterized by maxima in the UV or blue region of the visible spectrum. Vibronic structure is present in the spectra of both pyrrole-based ligands **K(2PyO)** and **K(2PyN)** with spacings of 4325 and 1278 cm^{-1}, respectively. The indole-aldehyde and indole-aldimine ligands show single broad bands at ca. 420 nm. All of the emission spectra overlap strongly with the absorption bands of these ligands with Stokes shifts in the range 45−85 nm (3100−6010 cm^{-1}), suggesting singlet $^1(\pi-\pi^*)$ emission.

The absorption spectra of the copper(I) complexes are each characterized by intense absorptions in the UV region. The highest energy bands in **1**−**4** are not apparent in the free ligands and are assigned as $\pi-\pi^*$ transitions of the ancillary phosphine ligands.[28] The lowest energy bands in complexes **1**−**4** have maxima at ca. 390 nm and show limited dependence on the identity of the phosphine or diphosphine ligand. Complexes **5** and **6** have maxima at ca. 285 nm with the spectrum of each complex exhibiting an additional low energy shoulder. In **5**, this shoulder is well-pronounced while, in **6**, it appears as a tail extending to 350 nm. Complex **7** displays a strong band at 337 nm and a low-energy, broad absorption at 432 nm. This low energy absorption is notably weaker with a molar extinction coefficient (ε) of 3400 M^{-1} cm^{-1}. The spectrum of **8** exhibits strong transitions at 261 and 370 nm with a shoulder at about 336 nm.

dx.doi.org/10.1021/ic2007588 |*Inorg. Chem.* 2011, 50, 7172–7188

Table 3. Crystal Data and Structure Refinement for 2PyN-H and Compounds 1−3

compound	2PyN-H	1	2	3
formula	$C_{11}H_{10}N_2$	$C_{48}H_{41}Cl_2CuN_2P_2$	$C_{41}H_{34}CuN_2O_{0.5}P_2$	$C_{48}H_{39}Cl_2CuN_2OP_2$
fw	170.21	842.21	688.18	856.19
T (K)	100.0(1)	100.0(1)	100.0(1)	100.0(1)
crystal system	orthorhombic	triclinic	monoclinic	triclinic
space group	*Pbca*	$P\bar{1}$	$P2_1/c$	$P\bar{1}$
a (Å)	9.3869(9)	10.0778(9)	16.631(3)	10.229(1)
b (Å)	18.119(2)	11.001(1)	26.069(4)	16.583(2)
c (Å)	21.187(2)	19.326(2)	17.111(3)	25.942(3)
α (deg)	90	103.585(2)	90	91.109(2)
β (deg)	90	91.243(2)	115.337(3)	94.510(2)
γ (deg)	90	103.576(2)	90	96.686(2)
V (Å^3)	3603.5(6)	2017.8(3)	6705(2)	4355.3(8)
Z	16	2	8	4
ρ_{calcd} (mg m^{-3})	1.255	1.386	1.363	1.306
μ (mm^{-1})	0.076	0.790	0.781	0.735
no. reflections collected	84197	45236	165018	67641
no. unique reflections	9638	18316	35726	24376
R_{int}[a]	0.0589	0.0676	0.0833	0.0593
no. observed reflections	6602	11178	21785	14846
no. parameters	315	496	866	1052
GOF[b] on F^2	1.042	1.011	1.052	1.021
$R1$[c] $[I > 2\sigma(I)]$	0.0502	0.0563	0.0541	0.0613
$wR2$[d]	0.1293	0.1188	0.1273	0.1510

[a] $R_{int} = |F_o^2 - \langle F_c^2\rangle|/|F_o^2|$. [b] GOF = $S = [[w(F_o^2 - F_c^2)^2]/(m - n)]^{1/2}$, where m = number of reflections and n = number of parameters. [c] $R1 = ||F_o| - |F_c||/|F_o|$. [d] $wR2 = [[w(F_o^2 - F_c^2)^2]/[w(F_o^2)^2]]^{1/2}$, where $w = 1/[2(F_o^2) + (aP)^2 + bP]$ and $P = {}^1/_3 \max(0, F_o^2) + {}^2/_3F_c^2$.

Table 4. Crystal Data and Structure Refinement for Compounds 5−8

compound	5	6	7	8
formula	$C_{42}H_{34}Cl_2CuNO_2P_2$	$C_{44}H_{36}CuNO_2P_2$	$C_{47}H_{38}Cl_4CuNO_2P_2$	$C_{51}H_{39}CuN_2OP_2$
fw	781.08	736.22	916.06	821.32
T (K)	100.0(1)	100.0(1)	100.0(1)	100.0(1)
crystal system	triclinic	tetragonal	monoclinic	triclinic
space group	$P\bar{1}$	$P4_2/n$	$P2_1/n$	$P\bar{1}$
a (Å)	9.657(1)	26.407(2)	9.483(1)	9.5399(7)
b (Å)	14.258(2)	26.407(2)	27.440(4)	10.8501(8)
c (Å)	14.593(2)	11.966(1)	16.305(3)	19.801(1)
α (deg)	88.946(2)	90	90	96.277(1)
β (deg)	74.641(2)	90	100.859(3)	94.581(1)
γ (deg)	71.779(2)	90	90	99.023(1)
V (Å^3)	1836.0(4)	8344.7(13)	4166.7(11)	2002.2(3)
Z	2	8	4	2
ρ_{calcd} (mg m^{-3})	1.413	1.172	1.460	1.362
μ (mm^{-1})	0.865	0.634	0.899	0.668
no. reflections collected	39666	200283	33657	44929
no. unique reflections	15924	22366	7426	18176
R_{int}[a]	0.0329	0.0547	0.1709	0.0385
no. observed reflections	12515	14350	4058	13432
no. parameters	461	493	514	514
GOF[b] on F^2	1.041	1.064	1.015	1.025
$R1$[c] $[I > 2\sigma(I)]$	0.0390	0.0552	0.0791	0.0446
$wR2$[d]	0.0975	0.1523	0.2077	0.1095

[a] $R_{int} = |F_o^2 - \langle F_o^2\rangle|/|F_o^2|$. [b] GOF = $S = [[w(F_o^2 - F_c^2)^2]/(m - n)]^{1/2}$, where m = number of reflections and n = number of parameters. [c] $R1 = ||F_o| - |F_c||/|F_o|$. [d] $wR2 = [[w(F_o^2 - F_c^2)^2]/[w(F_o^2)^2]]^{1/2}$, where $w = 1/[2(F_o^2) + (aP)^2 + bP]$ and $P = {}^1/_3 \max(0, F_o^2) + {}^2/_3F_c^2$.

dx.doi.org/10.1021/ic2007588 |*Inorg. Chem.* 2011, 50, 7172–7188

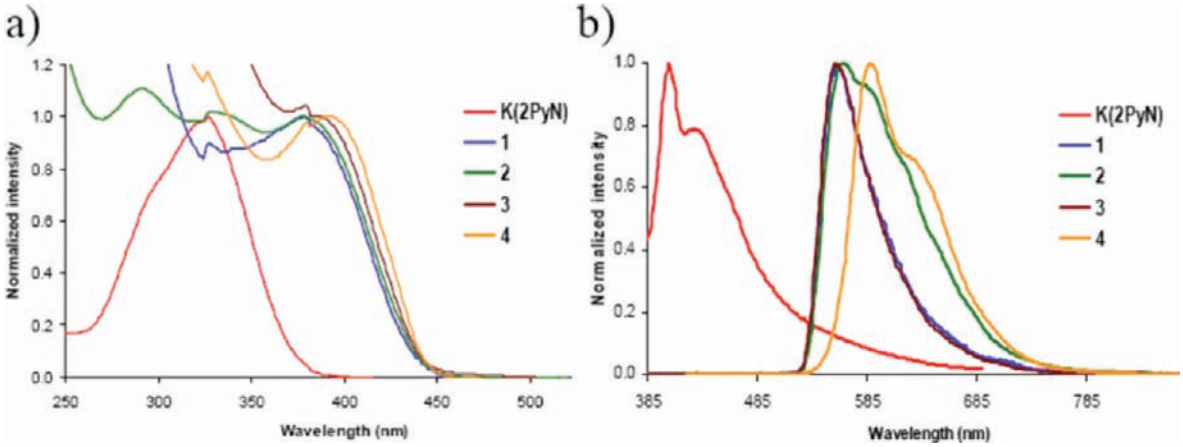

Figure 9. (a) Absorption and (b) emission spectra of **K(2PyN)** and the [Cu(2PyN)(diphosphine)] compounds **1**−**4** in fluid CH_2Cl_2 (1×10^{-5} M).

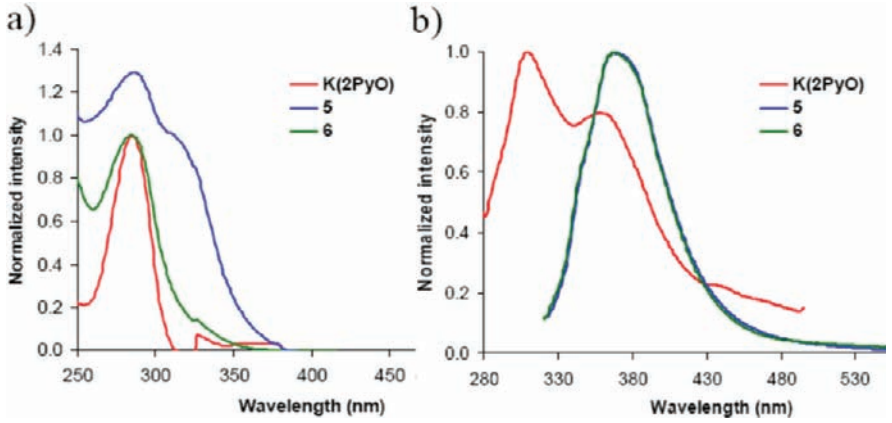

Figure 10. (a) Absorption and (b) emission spectra of **K(2PyO)** and the [Cu(2PyO)(diphosphine)] compounds **5**−**6** in fluid CH_2Cl_2 (1×10^{-5} M).

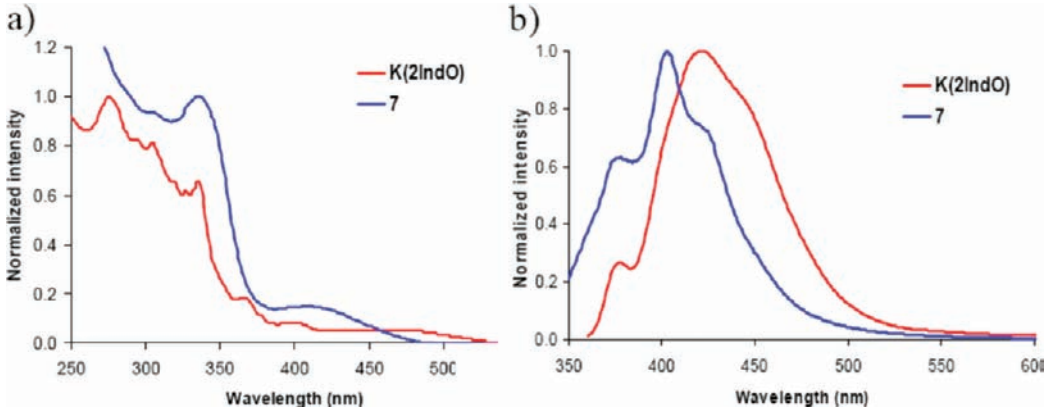

Figure 11. (a) Absorption and (b) emission spectra of **K(2IndO)** and [Cu(2IndO)(DPEPHOS)] (**7**) in fluid CH_2Cl_2 (1×10^{-5} M).

The solution emission spectra of complexes **1**−**4**, which all contain the **2PyN** ligand, are similar, with maxima near 590 and shoulders at 630 nm. Complexes **1** and **3** lack the vibronic structure observed in the free ligand. The spacing between peaks for complex **4** is 1080 cm^{-1}. With the exception of **4**, lifetimes are on the order of 70−2400 μs. The solution emission spectrum of complex **8**, which also possesses a (N,N), (P,P) donor set, exhibits dual emission with maxima at 560 and 680 nm with a lifetime of 65 μs for the low energy emission and a lifetime shorter than the limit of the phosphorimeter (~2 μs) for the high energy band. Excitation spectra were obtained while monitoring emission at both emission peaks. Both excitation spectra are characterized by strong maxima at 405 nm and weaker shoulders at 290 nm. The (N,O), (P,P) complexes **5** and **6** exhibit identical emission at 370 nm with lifetimes of <2 μs, while complex **7** exhibits a structured emission with a maximum at 403 nm and a lifetime of 10 μs.

dx.doi.org/10.1021/ic2007588 |*Inorg. Chem.* 2011, 50, 7172–7188

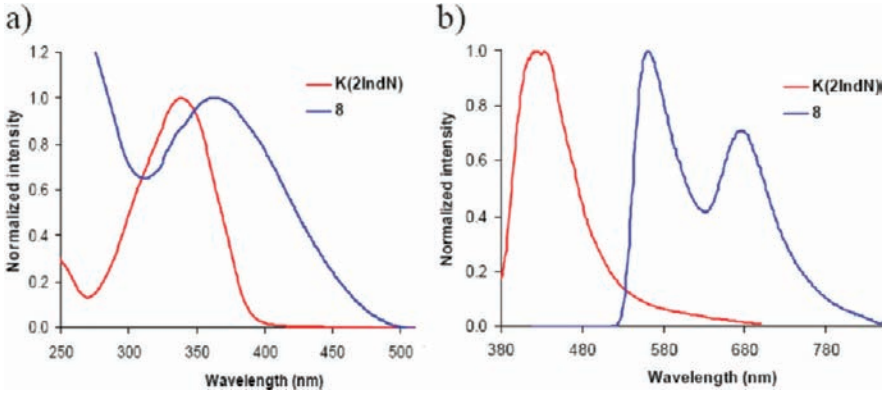

Figure 12. (a) Absorption and (b) emission spectra of **K(2IndN)** and [Cu(2IndN)(DPEPHOS)] (**8**) in fluid CH_2Cl_2 (1×10^{-5} M).

The excited states in **1**−**8** may be assigned by comparison of the complex and free ligand emission spectra in conjunction with lifetime data. For **4** the similar vibronic spacing between **K(2PyN)** and the complex is suggestive of strong contributions from ligand-based excited states in the complex. The large Stokes' shift and long lifetimes in each complex are consistent with triplet emissions. The emission maxima are marginally affected by the identity of the phosphine ligand, suggesting little participation of phosphine in the charge transfer state. Instead, we propose that the Cu(I) ion primarily helps to promote intersystem crossing (ISC) to the ligand-based $^3(\pi-\pi^*)$ emissive state although the absence of vibronic structure in **1** and **3** suggests some MLCT component. This assignment of $^3(\pi-\pi^*)$ contrasts with that made for zinc bis(pyrrole-aldimine) complexes, in which the radiative lifetimes are consistent with singlet fluorescence rather than triplet phosphorescence.[10b]

The absorption maxima of the pyrrole-aldehyde complexes **5** and **6** are identical to those of **K(2PyO)**, indicating little perturbation of the pyrrole-aldehyde ILCT absorption upon coordination to Cu, although the additional low energy shoulders may be indicative of a MLCT component. Emission spectra of **5** and **6** are red-shifted from that of the free **K(2PyO)** ligand and lack the vibronic structure present in the ligand emission, indicating some modification of the emissive state upon coordination to copper.

The UV region in the absorption spectrum of **7** is similar to that of **K(2IndO)** and is thus assigned as mainly a ligand-based $^1(\pi-\pi^*)$. However, a low energy band at 432 nm may be assigned as a metal-to-ligand charge transfer (MLCT) on the basis of its extinction coefficient ($\varepsilon = 3400\ M^{-1}\ cm^{-1}$) and by comparison to copper complexes in the literature.[6j,k] The maximum in the excitation spectrum of **7** of 336 nm is congruent with the maximum absorption, and excitation into this band results in emission that is slightly blue-shifted from that of **K(2IndO)**. This result may be due to slight differences in the indole-aldehyde π-orbital energies in the presence of K^+ or in the copper(I) complex.

The absorption at 261 nm in **8** is similar to those of **7** and **3** and is logically phosphine-based while the broad band at 370 nm has a high energy shoulder which overlaps with **K(2IndN)**. The shoulder can be assigned as **2IndN** $^1(\pi-\pi^*)$ while the maximum at 370 nm may contain some MLCT character. The emission of **8** is unique among complexes studied here insomuch as two emission bands with different lifetimes are observed, which is consistent with dual emission. The excitation spectra obtained while monitoring emission at both emission maxima are identical, with maxima at 405 and 290 nm. The lifetime of the higher energy band could not be measured, but the 680 nm emission lifetime is 9 μs. A possible assignment for the two bands is separate emission from ^{3}(MLCT) and $^3(\pi-\pi^*)$.

Spectroscopic Properties in Frozen Glass. The excitation and emission of the copper(I) compounds **1**−**8** were measured in frozen Me-THF at low temperature (77 K). Table 5 includes the emission data obtained from these measurements, and the spectra are shown in Figures 13 and 14.

The excitation bands of all the compounds at 77 K are approximate mirror images of their emission bands (see Figures 14 and 15). The emission spectra of **2PyN** derivatives are structured with maxima at 569 nm for **1** and 577 nm for **2**−**4**. The peaks are better defined than in solution, and the vibronic spacings are 1420 cm^{-1} and 1185 cm^{-1} for **1**, and 1458 cm^{-1} and 1253 cm^{-1} for **2**−**4**. Lifetimes in the frozen glass range from 2500 to 3600 μs. The emission of complex **8** is similar in vibronic progression to those of **1**−**4**, with spacings of 1328 cm^{-1} and 1144 cm^{-1}. The emission maximum at 622 nm is significantly red-shifted from those of the other complexes with N,N ligands by ca. 45 nm, which is attributed to the delocalization of the frontier orbitals onto the conjugated indole ring. For **1**−**4** and **8**, the similar structure in solution and frozen glass and the long luminescence lifetimes support an assignment of ligand-based triplet emission, $^3(\pi-\pi^*)$.

In the frozen glass, the emission spectra of **5** and **6** are nearly identical, with maxima at 502−504 nm and shoulders at 472−473 nm. The luminescence lifetimes of both complexes are 1800 μs. The spectrum of **7** is broad with $\lambda_{max} = 436$ nm and a lifetime of 730 μs. Complexes **5** and **6** differ only in the identity of the diphosphine, and their identical emission at 77 K corroborates conclusions made in the solution phase regarding the emission assignment as ^{3}(MLCT + $\pi-\pi^*$).

Spectroscopic Properties in Solid State. The emission spectra of **1**−**8** were measured in the solid state at 298 K (Figure 15) and at 77 K (Figure 16). Powder samples were packed in glass capillary tubes.

The spectra of **1**−**4** and **8** exhibit the same type of vibronic structure seen in solution and frozen glass samples. At 298 K, the emission maxima of the **2PyN**- and **2IndN**-supported complexes are similar to those of solution samples, with slight variations between complexes (Figure 16a). Upon cooling to 77 K, the emission of **1** blue shifts, while **2**−**4** exhibit slightly red-shifted spectra. Lifetimes on the order of 100−1400 μs at room temperature are somewhat longer at 77 K. The similarities between solid state and dilute solution emission data suggest

dx.doi.org/10.1021/ic2007588 |*Inorg. Chem.* 2011, 50, 7172–7188

Table 5. Absorption and Emission Data of K(L_2) Ligands and Compounds 1−8

compound	media	absorptions[a], λ_{max}/nm (ε/M^{-1} cm^{-1})	excitation, λ_{ex}/nm	emission, λ_{em}/nm (τ/μs)[d]	Stokes' shift[b]/nm (cm^{-1})	Φ_{em}[c], %
K(2PyO)	CH_2Cl_2	285 (12800)	262	310	48 (5910)	0.54
K(2PyN)	CH_2Cl_2	326 (26650)	359	404	45 (3103)	0.09
K(2IndO)	CH_2Cl_2	276 (9225), 306 (8000), 321 (6175), 336 (5850), 370 (1650), 408 (850)	336	421	85 (6009)	28
K(2IndN)	CH_2Cl_2	338 (34000)	365	423	58 (3757)	0.19
1	CH_2Cl_2	258 (25750), 379 (8550)	366	556 (2400)	190 (9337)	0.02
	2-Me-THF, 77 K			569 (3600)		
	solid, 298 K			589 (1400)		
	solid, 77 K			597 (3100)		
2	CH_2Cl_2	289 (19550), 343 (21500), 379 (27225)	328	564	236 (12757)	0.12
	2-Me-THF, 77 K			577 (2600)		
	solid, 298 K			591 (520)		
	solid, 77 K			601 (1500)		
3	CH_2Cl_2	284 (18875), 327 (14975), 386 (16450)	366	556 (210)	190 (9337)	0.02
	2-Me-THF, 77 K			577 (2600)		
	solid, 298 K			586 (900)		
	solid, 77 K			595 (2300)		
4	CH_2Cl_2	288 (25050), 392 (23250)	399	589 (70)	190 (8085)	0.26
	2-Me-THF, 77 K			577 (2500)		
	solid, 298 K			593 (190)		
	solid, 77 K			615 (1100)		
5	CH_2Cl_2	287 (19250), 312 (21825)	314	370[e]	56 (4820)	2.9
	2-Me-THF, 77 K			502 (1800)		
	solid, 298 K			587 (3000)		
	solid, 77 K			577 (2700)		
6	CH_2Cl_2	287 (23625)	312	368[e]	56 (4877)	2.8
	2-Me-THF, 77 K			504 (2500)		
	solid, 298 K			560 (10)		
	solid, 77 K			425 (250)		
				524 (530, 50)[f]		
7	CH_2Cl_2	337 (23425), 432 (3400)	336	403 (10)	67 (4948)	1.6
	2-Me-THF, 77 K			436 (730)		
	solid, 298 K			370[e]		
	solid, 77 K			457 (480)		
8	CH_2Cl_2	261 (36625), 336 (20975), 370 (27750)	405	560, 680 (65)	155 (6834), 275 (985)	0.06
	2-Me-THF, 77 K			622 (470)		
	solid, 298 K			611 (85)		
	solid, 77 K			615 (470)		

[a] Solution concentration ~ 10^{-5} M. [b] Measured as the difference between maxima of excitation and emission. [c] Measured in CH_2Cl_2 relative to $[Ru(bpy)_3]^+$ in air-equilibrated water (Φ_R = 0.028).[17] [d] Fluorescence-decay curves are included in Figures S35−S38 of the Supporting Information. [e] Lifetime less than 2 μs. [f] Fit to a biexponential decay.

that the emission is insensitive to aggregation and that molecular emission is observed in the solid state. Structured emission is observed for **8** with λ_{max} = 611 nm at 298 K and 615 nm at 77 K.

At 298 K, the spectra of **5** and **6** are similar, with maxima at 587 and 560 nm, respectively. Upon cooling, two bands at 425 and 524 nm are evident in **6** while the band in **5** is only slightly blue-shifted. The two emission bands in **6** have unique excitation spectra and different lifetimes, suggesting possible emission from aggregation states in the solid state at low temperature. The large blue shift of the maximum in **6** may indicate emission from a higher energy T_N state as a result of slow relaxation to T_1 at 77 K. Complex **7** emits at 370 nm at 298 K and 457 nm at 77 K.

Molecular Orbital Calculations. To further examine the excited states in these complexes, DFT calculations at the B3LYP/6-31+G level of theory as implemented in Gaussian 09[29] were performed on the singlet ground states (S_0) of complexes **3**, **5**, **7**, and **8** as representative examples that vary in the (N,N) or (N,O) ligands and are consistent in the diphosphine

dx.doi.org/10.1021/ic2007588 |*Inorg. Chem.* 2011, 50, 7172–7188

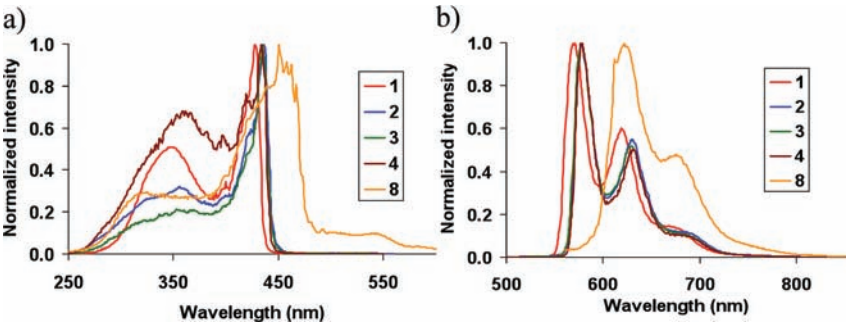

Figure 13. (a) Excitation and (b) emission spectra of compounds **1**−**4** and **8** in frozen Me-THF at 77 K.

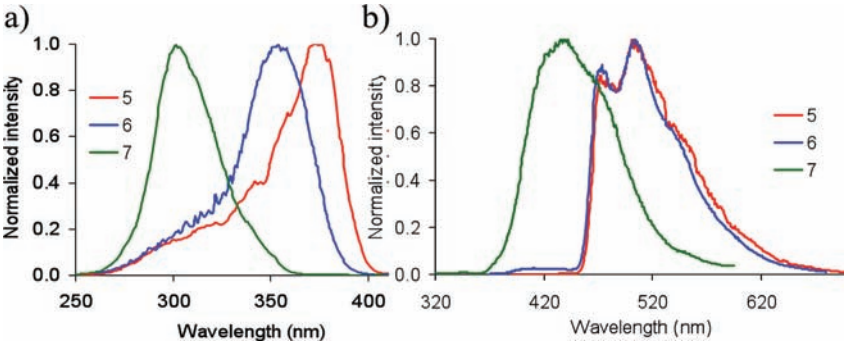

Figure 14. (a) Excitation and (b) emission spectra of compounds **5**, **6**, and **7** in frozen Me-THF at 77 K.

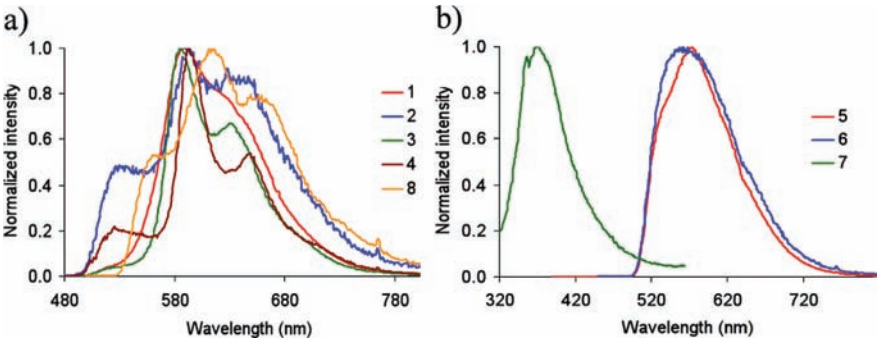

Figure 15. Emission spectra of compounds (a) **1**−**4** and **8** and (b) **5**−**7** in solid-state at 298 K.

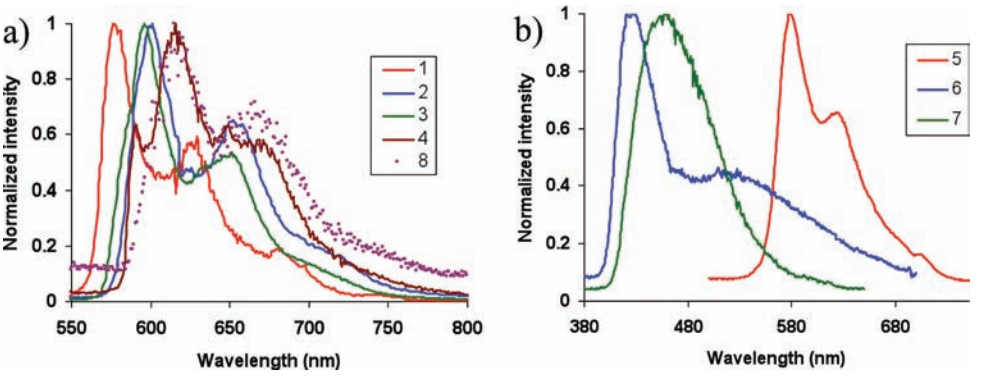

Figure 16. Phosphorescence emission spectra of compounds (a) **1**−**4** and **8** and (b) **5**−**7** in solid-state at 77 K. Spectra were obtained after a 0.01 ms delay and are the average of five consecutive scans.

(DPEPHOS). The optimized geometries of **3** and **8** are similar to the X-ray structures, but the calculated geometries of **5** and **7** differ somewhat from experimentally determined structures. The main difference is an elongation of the Cu−O bond length, with a

dx.doi.org/10.1021/ic2007588 |*Inorg. Chem.* 2011, 50, 7172–7188

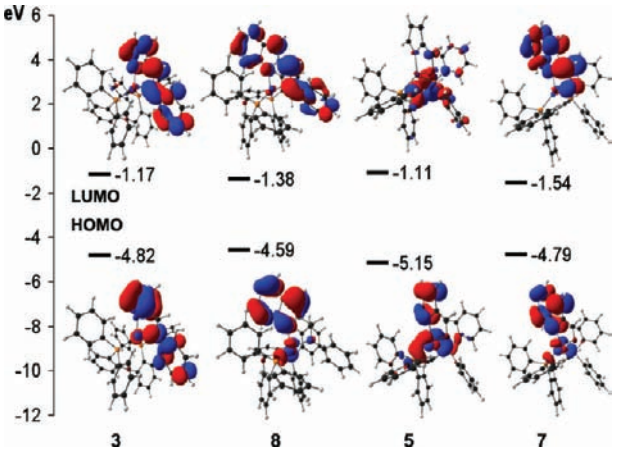

Figure 17. Diagrams and energies (eV) of the HOMO and LUMO for complexes **3**, **8**, **5**, and **7**. Isovalue = 0.05.

consequential flattening of the tetrahedral geometry toward pyramidal coordination. Coordinates for the calculated geometry in *xyz* format are provided in the Supporting Information.

Diagrams of the HOMO and LUMO for each complex are shown in Figure 17. Additional frontier orbital diagrams are included in the Supporting Information.

In each complex, the HOMO is comprised primarily of pyrrole or indole π functions mixed to varying degrees with Cu-d character. For complexes **3**, **8**, and **7**, the LUMO is delocalized over π^* orbitals of the anionic ligand while the LUMO of **5** is localized on the aryl moieties of the DPEPHOS backbone. The different nature of the LUMO calculated for **5** was viewed with some concern; therefore, time-dependent calculations were performed for **5** and **7** to better model the electronic transitions in these complexes. Complete results of these calculations are included in the Supporting Information, and the lowest energy singlet and triplet transitions, along with energies, oscillator strengths, and major orbital contributions, are given in Table 6.

In **7**, the T_1 and S_1 absorptions are exclusively HOMO → LUMO excited states ($\pi-\pi^*$). The two lowest singlet absorptions in complex **5** were found to be transitions from mixed HOMO and HOMO−2 orbitals to mixed LUMO and LUMO+2 orbitals. The HOMO−2 level is largely copper-localized while LUMO+2 is the lowest π^* level of the pyrrole-aldehyde (Supporting Information). The lowest triplet absorption, which would correspond in character to an emissive triplet state, is a HOMO−1 → LUMO+2 transition. The latter is identified as pyrrole-aldehyde $^3(\pi-\pi^*)$ and is consistent with **3**, **8**, and **7**. Apparently the relative energies of phosphine and pyrrole π^* orbitals in these complexes are highly sensitive to subtle modifications of the anionic ligand. In related work, we have observed that the electronic modification of a triazole ring changes the emissive state from predominately intraligand to interligand charge transfer.[8]

Analyzed in the context of experimental data, the molecular orbital calculations reinforce the unifying theme that the photophysical properties of these complexes depend largely on the identity of the anionic ligands and less upon differences in the supporting diphosphine. Complexes **1**−**4** and **8** with (N,N) pyrrole or indole ligands form a congruent series with similar behavior in solution, in frozen glass, or in the solid state. The lower energy emission in **8** is interpreted as a result of charge delocalization in the LUMO and was modeled well by DFT. A similar comparison of pyrrole-aldehyde complexes **5** and **6** vs indole-aldehyde complex **7** is not as straightforward. Complex **7** emits lower energy in solution but emits higher energy in the solid state or frozen glass, and simple indole delocalization arguments are not sufficient. Close examination of the molecular orbitals for the emissive states reveals that the HOMO → LUMO transition of **7** contains significant Cu-d character (MLCT + $\pi-\pi^*$) and no participation of aldehyde lone pairs in the HOMO. Conversely, the HOMO−1 → LUMO+1 triplet state in complex **5** has minimal Cu-character and extensive oxygen lone pair contribution. Thus, emission in **5** and **6** is more appropriately described as $^3(n-\pi^* + \pi-\pi^*)$.

Table 6. Lowest Energy Electronic Transitions for 5 and 7 Calculated by TD-DFT

complex	transition	energy (cm^{-1})	wavelength (nm)	oscillator strength	major contributions
5	T_1	21820	458.3	0	H−1 → L+2 (95%)
	S_1	27395	365.0	0.0265	HOMO → LUMO (45%)
					H−2 → L+2 (30%)
					HOMO → L+2 (10%)
	S_2	27548	363.0	0.0131	HOMO → LUMO (34%)
					H−2 → L+2 (47%)
7	T_1	15004	666.5	0	HOMO → LUMO (100%)
	S_1	21740	460.0	0.0687	HOMO → LUMO (86%)

Conclusions. A series of neutral luminescent copper(I) complexes of the types [Cu(N,N)(P,P)] and [Cu(N,O)(P,P)], containing phosphine or diphosphines and coordinated pyrrole- or indole-aldimine or aldehyde ligands, was prepared and structurally characterized, and the photophysical properties of the complexes were established in solution, the solid state, and frozen glasses. The complexes are all thermally stable and exhibit long-lived emission, the excited states of which have been assigned as mixed intraligand and metal-to-ligand charge transfer ^{3}(MLCT + $\pi-\pi^*$) transitions. The experimental results are consistent with the conclusions drawn from quantum chemical calculations, the latter of which demonstrate a large dependence of the photophysical properties of these complexes on the identity of the (N,N) or (N,O) anionic ligands. In the case of the aldimine-derived compounds, **1**−**4** and **8**, the experimental results show that the emission is insensitive to aggregation and, thus, molecular emission—a desired property for OLED emitters—is observed. Furthermore, compounds **2**−**4** can be sublimed at T = 230−250 °C under vacuum and, in turn, give proof for this class of (N,N) compounds as potential candidates for chemical vapor deposition (CVD) processes.

■ ASSOCIATED CONTENT

Supporting Information. Selected NMR spectra, additional structural information, fluorescence decay plots, frontier orbital diagrams, calculated electronic transition energies, relevant orbitals for the four lowest singlet and triplet states in compounds **3**, **5**, **7**, and **8**, and *xyz* coordinates for calculated geometries. This material is available free of charge via the Internet at http://pubs.acs.org.

■ AUTHOR INFORMATION

Corresponding Author

*E-mail: eisenberg@chem.rochester.edu.

■ ACKNOWLEDGMENT

The authors thank the National Science Foundation (NSF-GOALI, Grant CHE-0616782) for the financial support to this work. We thank Dr. Joseph Deaton (Dept. of Chemistry, Bowling Green State University), Dr. Henry J. Gysling, and Prof. David R. McMillin (Dept. of Chemistry, Purdue University) for very helpful discussions.

■ REFERENCES

(1) (a) So, F.; Shi, J. *Opt. Sci. Eng.* **2008**, *133*, 351. (b) Wong, T. K. S. In *Handbook of Organic Electronics and Photonics*; Nalwa, H. S., Eds.; American Scientific Publishers: Stevenson Ranch, CA, 2008; Vol. 2, pp 413−472. (c) Shinar, J.; Shinar, R. *J. Phys. D: Appl. Phys.* **2008**, *41*, 133001.

(2) For the classic example of construction of an OLED, refer to: Tang, C. W.; VanSlyke, S. A. *Appl. Phys. Lett.* **1987**, *51*, 913–915.

(3) (a) Baldo, M. A.; O'Brien, D. F.; You, Y.; Shoustikov, A.; Sibley, S.; Thompson, M. E.; Forrest, S. R. *Nature (London)* **1998**, *395*, 151. (b) O'Brien, D. F.; Baldo, M. A.; Thompson, M. E.; Forrest, S. R. *Appl. Phys. Lett.* **1999**, *74*, 442–444. (c) Baldo, M. A.; Lamansky, S.; Burrows, P. E.; Thompson, M. E.; Forrest, S. R. *Appl. Phys. Lett.* **1999**, *75*, 4–6. (d) Adachi, C.; Baldo, M. A.; Forrest, S. R.; Thompson, M. E. *Appl. Phys. Lett.* **2000**, *77*, 904–906. (e) Adachi, C.; Baldo, M. A.; Thompson, M. E.; Forrest, S. R. *J. Appl. Phys.* **2001**, *90*, 5048–5051.

(4) (a) Deaton, J. C.; Young, R. H.; Lenhard, J. R.; Rajeswaran, M.; Hou, S. *Inorg. Chem.* **2010**, *49*, 9151–9161. (b) Vezzu, D. A. K.; Deaton, J. C.; Jones, J. S.; Bartolotti, L.; Harris, C. F.; Marchetti, A. P.; Kondakova, M.; Pike, R. D.; Hou, S. *Inorg. Chem.* **2010**, *49*, 5107–5119. (c) Sajoto, T.; Djurovich, P. I.; Tamayo, A.; Oxgaard, J.; Goddard, W. A.; Thompson, M. E. *J. Am. Chem. Soc.* **2009**, *131*, 9813–9822. (d) *Highly Efficient OLEDs with Phosphorescent Materials*; Yersin, H., Ed.; Wiley-VCH Verlag GmbH & Co., KgaA: Weinheim, Germany, 2008. (e) Sun, Y.; Borek, C.; Hanson, K.; Djurovich, P. I.; Thompson, M. E.; Brooks, J.; Brown, J. J.; Forrest, S. R. *Appl. Phys. Lett.* **2007**, *90*, 213503-1–3. (f) Dedeian, K.; Shi, J.; Forsythe, E.; Morton, D. C. *Inorg. Chem.* **2007**, *46*, 1603–1611. (g) Dedeian, K.; Shi, J.; Shepherd, N.; Forsythe, E.; Morton, D. C. *Inorg. Chem.* **2005**, *44*, 4445–4447. (h) Sajoto, T.; Djurovich, P. I.; Tamayo, A.; Yousufuddin, M.; Bau, R.; Thompson, M. E. *Inorg. Chem.* **2005**, *44*, 7992–8003. (i) He, G.; Schneider, O.; Qin, D.; Zhou, X.; Pfeiffer, M.; Leo, K. *J. Appl. Phys.* **2004**, *95*, 5773–5777. (j) Tsuboyama, A.; Iwawaki, H.; Furugori, M.; Mukaide, T.; Kamatani, J.; Igawa, S.; Moriyama, T.; Miura, S.; Takiguchi, T.; Okada, S.; Hoshino, M.; Ueno, K. *J. Am. Chem. Soc.* **2003**, *125*, 12971–12979. (k) Brooks, J.; Babayan, Y.; Lamansky, S.; Djurovich, P. I.; Tsyba, I.; Bau, R.; Thompson, M. E. *Inorg. Chem.* **2002**, *41*, 3055–3066. (l) D'Andrade, B. W.; Thompson, M. E.; Forrest, S. R. *Adv. Mater.* **2002**, *14*, 147–151. (m) Wang, Y.; Herron, N.; Grushin, V. V.; LeCloux, D.; Petrov, V. *Appl. Phys. Lett.* **2001**, *79*, 449–451. (n) Lamansky, S.; Djurovich, P.; Murphy, D.; Abdel-Razzaq, F.; Lee, H. E.; Adachi, C.; Burrows, P. E.; Forrest, S. R.; Thompson, M. E. *J. Am. Chem. Soc.* **2001**, *123*, 4304–4312. (o) Lamansky, S.; Djurovich, P.; Murphy, D.; Abdel-Razzaq, F.; Kwong, R.; Tsyba, I.; Bortz, M.; Mui, B.; Bau, R.; Thompson, M. E. *Inorg. Chem.* **2001**, *40*, 1704–1711. (p) King, K. A.; Spellane, P. J.; Watts, R. J. *J. Am. Chem. Soc.* **1985**, *107*, 1431–1432.

(5) Barbieri, A.; Accorsi, G.; Armaroli, N. *Chem. Commun.* **2008**, 2185–2193.

(6) (a) Liu, Z.; Qayyum, M. F.; Wu, C.; Whited, M. T.; Djurovich, P. I.; Hodgson, K. O.; Hedman, B.; Solomon, E. I.; Thompson, M. E. *J. Am. Chem. Soc.* **2011**, *133*, 3700–3703. (b) Deaton, J. C.; Switalski, S. C.; Kondakov, D. Y.; Young, R. H.; Pawlik, T. D.; Giesen, D. J.; Harkins, S. B.; Miller, A. J. M.; Mickenberg, S. F.; Peters, J. C. *J. Am. Chem. Soc.* **2010**, *132*, 9499–9508. (c) Si, Z.; Li, J.; Li, B.; Liu, S.; Li, W. *J. Lumin.* **2009**, *129*, 181–186. (d) Zhang, L.; Li, B.; Su, Z. *J. Phys. Chem. C* **2009**, *113*, 13968–13973. (e) Zhang, Q.; Ding, J.; Cheng, Y.; Wang, L.; Xie, Z.; Jing, X.; Wang, F. *Adv. Funct. Mater.* **2007**, *17*, 2983–2990. (f) Armaroli, N.; Accorsi, G.; Cardinalli, F.; Listorti, A. *Top. Curr. Chem.* **2007**, *280*, 69–115. (g) Moudam, O.; Kaeser, A.; Delavaux-Nicot, B.; Duhayon, C.; Holler, M.; Accorsi, G.; Armaroli, N.; Séguy, I.; Navarro, J.; Destruel, P.; Nierengarten, J.-F. *Chem. Commun.* **2007**, 3077–3079. (h) Tsuboyama, A.; Kuge, K.; Furugori, M.; Okada, S.; Hoshino, M.; Ueno, K. *Inorg. Chem.* **2007**, *46*, 1992–2001. (i) Che, G.; Su, Z.; Li, W.; Chu, B.; Li, M.; Hu, Z.; Zhang, Z. *Appl. Phys. Lett.* **2006**, *89*, 103511–103513. (j) McCormick, T.; Jia, W.-L.; Wang, S. *Inorg. Chem.* **2006**, *45*, 147–155. (k) Jia, W.-L.; McCormick, T.; Tao, Y.; Lu, J.-P.; Wang, S. *Inorg. Chem.* **2005**, *44*, 5706–5712. (l) Zhang, Q.; Zhou, Q.; Cheng, Y.; Wang, L.; Ma, D.; Jing, X.; Wang, F. *Adv. Mater.* **2004**, *16*, 432–436. (m) Ma, Y.; Che, C.-M.; Chao, H.-Y.; Zhou, X.; Chan, W.-H.; Shan, J. *Adv. Mater.* **1999**, *11*, 852–857.

(7) (a) Kuang, S.-M.; Cuttell, D. G.; McMillin, D. R.; Fanwick, P. E.; Walton, R. A. *Inorg. Chem.* **2002**, *41*, 3313–3322. (b) Cuttell, D. G.; Kuang, S.-M.; Fanwick, P. E.; McMillin, D. R.; Walton, R. A. *J. Am. Chem. Soc.* **2002**, *124*, 6–7.

(8) Manbeck, G. F.; Brennessel, W. W.; Eisenberg, R. *Inorg. Chem.* **2011**, *50*, 3431–3441.

(9) Grushin, V. V.; Marshall, W. J. *Adv. Synth. Catal.* **2004**, *346*, 1457–1460.

(10) (a) Gomes, C. S. B.; Suresh, D.; Gomes, P. T.; Veiros, L. F.; Duarte, M. T.; Nunes, T. G.; Oliveira, M. C. *Dalton Trans.* **2010**, *39*, 736–748. (b) Gomes, C. S. B.; Gomes, P. T.; Duarte, M. T.; Di Paolo, R. E.; Maçanita, A. L.; Calhorda, M. J. *Inorg. Chem.* **2009**, *48*, 11176–11186. (c) Bellabarba, R. M.; Gomes, P. T.; Pascu, S. I. *Dalton Trans.* **2003**, 4431–4436. For additional references on the preparation of bis(iminopyrrolyl) compounds, consult the following: (d) Carabineiro, S. A.; Bellabarba, R. M.; Gomes, P. T.; Pascu, S. I.; Veiros, L. F.; Freire, C.; Pereira, L. C. J.; Henriques, R. T.; Oliveira, M. C.; Warren, J. E. *Inorg. Chem.* **2008**, *47*, 8896–8911. (e) Carabineiro, S. A.; Silva, L. C.; Gomes, P. T.; Pereira, L. C. J.; Veiros, L. F.; Pascu, S. I.; Duarte, M. T.; Namorado, S.; Henriques, R. T. *Inorg. Chem.* **2007**, *46*, 6880–6890. (f) Carabineiro, S. A.; Gomes, P. T.; Veiros, L. F.; Freire, C.; Pereira, L. C. J.; Henriques, R. T.; Warren, J. E.; Pascu, S. I. *Dalton Trans.* **2007**, 5460–5470. For references concerning the coordination of pyrrole-aldimine ligands to transition metals reported by other groups, consult the following: (g) Li, Y.-S.; Li, Y.-R.; Li, X.-F. *J. Organomet. Chem.* **2003**, *667*, 185–191. (h) Iverson, C. N.; Carter, C. A. G.; Baker, R. T.; Scollard, J. D.; Labinger, J. A.; Bercaw, J. E. *J. Am. Chem. Soc.* **2003**, *125*, 12674–12675 .(i) Yoshida, Y.; Matsui, S.; Takagi, Y.; Mitani, M.; Nakano, T.; Tanaka, H.; Kashiwa, N.; Fujita, T. *Organometallics* 2001, *20*, 4793–4799and ref 9.For a review on the use of pyrrolate-aldimines on copper(II) complexes, refer to the following: (j) Wansapura, C. M.; Juyoung, C.; Simpson, J. L.; Szymanski, D.; Eaton, G. R.; Eaton, S. S.; Fox, S. *J. Coord. Chem.* **2003**, *56*, 975–993. For very early references regarding the use of this type of ligand over copper(II), refer to the following: (k) Addison, A. W.; Stenhouse, J. H. *Inorg. Chem.* **1978**, *17*, 2161–2165. (l) Wei, C. W. *Inorg. Chem.* **1972**, *11*, 2315–2321. (m) Tewari, R.; Srivastava, R. C. *Acta Crystallogr.* **1971**, *B27*, 1644–1649. (n) Yeh, K.-N.; Barker, R. H. *Inorg. Chem.* **1967**, *6*, 830–833. For a reference on the preparation of photoluminescent copper(I)-phosphine complexes with (N,O) ligands, refer to the following: (o) Li, D.; Li, R.-Z.; Ni, Z.; Qi, Z.-Y.; Feng, X.-L.; Cai, J.-W. *Inorg. Chem. Commun.* **2003**, *6*, 469–473.

(11) A study on the use of similar ligands, 2-(2-pyridyl)indole and 2-(2-pyridyl)-7-azaindole, for the preparation of luminescent zinc(II), berilium(II), and boron(III) compounds has been reported in the following:Liu, S.-F.; Wu, Q.; Schmider, H. L.; Aziz, H.; Hu, N.-X.; Popović, Z.; Wang, S. *J. Am. Chem. Soc.* **2000**, *122*, 3671–3678. For a reference on the crystal structure of the related *N*-phenyl-2-(phenyliminomethyl)pyrrole-1-carboxamide, consult the following:Imhof, W. *Acta Crystallogr.* **2007**, *E63*, o4265.

(12) Pangborn, A. B.; Giardello, M. A.; Grubbs, R. H.; Rosen, R. K.; Timmers, F. J. *Organometallics* **1996**, *15*, 1518–1520.

(13) Errington, R. J. *Advanced Practical Inorganic and Metalorganic Chemistry*; Blackie Academic & Professional: U.K., 1997; pp 97− 101.

(14) Gysling, H. J. In *Inorganic Syntheses*; Shriver, D. F., Ed.; John Wiley & Sons: New York, 1979; Vol. XIX, pp 92−94.

(15) Demas, J. N.; Crosby, G. A. *J. Phys. Chem.* **1971**, *75*, 991–1024.

(16) Thoi, V. S.; Stork, J. R.; Magde, D.; Cohen, S. M. *Inorg. Chem.* **2006**, *45*, 10688–10697.
(17) (a) Lazarides, T.; Tart, N. M.; Sykes, D.; Faulkner, S.; Barbieri, A.; Ward, M. D. *Dalton Trans.* **2009**, *20*, 3971–3979. (b) Nakamaru, K. *Bull. Chem. Soc. Jpn.* **1982**, *55*, 2697–2705.
(18) Grushin, V. V.; Marshall, W. J. *Adv. Synth. Catal.* **2004**, *346*, 1457–1460.
(19) *APEX2*, version 2009.3-0; Bruker AXS: Madison, WI, 2009.
(20) Sheldrick, G. M. *SADABS*, version 2008/1; University of Göttingen: Göttingen, Germany, 2008.
(21) *SAINT*, version 7.60A; Bruker AXS: Madison, WI, 2008.
(22) Altomare, A.; Burla, M. C.; Camalli, M.; Cascarano, G. L.; Giacovazzo, C.; Guagliardi, A.; Moliterni, A. G. G.; Polidori, G.; Spagna, R. *SIR97: A new program for solving and refining crystal structures*; Instituto di Cristallografia, CNR: Bari, Italy, 1999.
(23) Sheldrick, G. M. *Acta Crystallogr.* **2008**, *A64*, 112–122.
(24) Spek, A. L. *PLATON: A multipurpose crystallographic tool, version 300106*; Utrecht University: Utrecht, The Netherlands, 2006.
(25) Yeh, K.-N.; Barker, R. H. *Inorg. Chem.* **1967**, *6*, 830–833.
(26) The dimerization of phenanthrene-iminopyrrole molecules resulting from hydrogen bonding interactions in addition to π-stacking of the phenanthrene rings in such molecules has been reported; see ref 10b.
(27) (a) Jardine, F. H.; Rule, L.; Vohra, A. G. *J. Chem. Soc. A* **1970**, 238–240. The formation of higher nuclearity copper(I) and silver(I) halide clusters by the addition of a diphosphine to neutral MX (M = Ag, Cu; X = Cl, Br, I) has been reported as well; see the following: (b) Nicola, C. D.; Effendy; Fazaroh, F.; Pettinari, C.; Skelton, B. W.; Somers, N.; White, A. H. *Inorg. Chim. Acta* **2005**, *358*, 720–734. (c) Effendy; Nicola, C. D.; Fianchini, M.; Pettinari, C.; Skelton, B. W.; Somers, N.; White, A. H. *Inorg. Chim. Acta* **2005**, *358*, 763–795.
(28) Aslandis, P.; Cox, P. J.; Tsipis, A. C. *Dalton Trans.* **2010**, *39*, 10238–10248.
(29) Frisch, M. J.; Trucks, G. W.; Schlegel, H. B.; Scuseria, G. E.; Robb, M. A.; Cheeseman, J. R.; Montgomery, J. A., Jr.; Vreven, T.; Kudin, K. N.; Burant, J. C.; Millam, J. M.; Iyengar, S. S.; Tomasi, J.; Barone, V.; Mennucci, B.; Cossi, M.; Scalmani, G.; Rega, N.; Petersson, G. A.; Nakatsuji, H.; Hada, M.; Ehara, M.; Toyota, K.; Fukuda, R.; Hasegawa, J.; Ishida, M.; Nakajima, T.; Honda, Y.; Kitao, O.; Nakai, H.; Klene, M.; Li, X.; Knox, J. E.; Hratchian, H. P.; Cross, J. B.; Bakken, V.; Adamo, C.; Jaramillo, J.; Gomperts, R.; Stratmann, R. E.; Yazyev, O.; Austin, A. J.; Cammi, R.; Pomelli, C.; Ochterski, J. W.; Ayala, P. Y.; Morokuma, K.; Voth, G. A.; Salvador, P.; Dannenberg, J. J.; Zakrzewski, V. G.; Dapprich, S.; Daniels, A. D.; Strain, M. C.; Farkas, O.; Malick, D. K.; Rabuck, A. D.; Raghavachari, K.; Foresman, J. B.; Ortiz, J. V.; Cui, Q.; Baboul, A. G.; Clifford, S.; Cioslowski, J.; Stefanov, B. B.; Liu, G.; Liashenko, A.; Piskorz, P.; Komaromi, I.; Martin, R. L.; Fox, D. J.; Keith, T.; Al-Laham, M. A.; Peng, C. Y.; Nanayakkara, A.; Challacombe, M.; Gill, P. M. W.; Johnson, B.; Chen, W.; Wong, M. W.; Gonzalez, C.; Pople, J. A.*Gaussian 03*, Revision C.02; Gaussian, Inc.: Wallingford, CT, 2004.